# A SAFETY AND DYNAMICS ANALYSIS OF THE SUBCRITICAL ADVANCED BURNER REACTOR: SABR

A Thesis
Presented to
The Academic Faculty

by

Tyler S. Sumner

In Partial Fulfillment
of the Requirements for the Degree
Master of Science in
Nuclear Engineering

School of Mechanical Engineering
Georgia Institute of Technology
August 2008

# A SAFETY AND DYNAMICS ANALYSIS OF THE SUBCRITICAL ADVANCED BURNER REACTOR: SABR

Approved by:

Dr. Willem F. G. van Rooijen, Advisor
School of Mechanical Engineering
*Georgia Institute of Technology*

Dr. Weston M. Stacey
School of Mechanical Engineering
*Georgia Institute of Technology*

Dr. Seyed M. Ghiaasiaan
School of Mechanical Engineering
*Georgia Institute of Technology*

Date Approved: May, 12 2008

## ACKNOWLEDGEMENTS

I would like to thank everyone that assisted me with this project, specifically Chris Sommer, my committee members, Dr. Ghiaasiaan and Dr. Stacey, and my advisor, Dr. van Rooijen. I could not have done this without your help. I would also like to thank my friends and my family, especially my parents for their limitless support in whatever I do.

# TABLE OF CONTENTS

## LIST OF TABLES

## LIST OF FIGURES

# SUMMARY

As the United States expands its quantity of nuclear reactors in the near future, the amount of spent nuclear fuel (SNF) will also increase. closing the nuclear fuel cycle has become the next major technical challenge for the nuclear energy industry. By separating the transuranics (TRU) from the SNF discharged by Light Water Reactors, it is possible to fuel Advanced Burner Reactors to minimize the amount of SNF that must be stored in High Level Waste Repositories.

One such ABR concept is the Subcritical Advanced Burner Reactor (SABR) being developed at the Georgia Institute of Technology. SABR is a subcritical, sodium-cooled fast reactor with a fusion neutron source capable of burning up to 25% of the TRU fuel over an 8.2 year residence time. In the SABR concept an annular core with a thickness of 0.6 m and an active height of 3.2 m surrounds the toroidal fusion neutron source. Neutron multiplication varies during the lifetime of the reactor from $k_{eff} = 0.95$ at the beginning of reactor life to 0.83 at the end of an equilibrium fuel cycle. Sixteen control rods worth \$9 are symmetrically positioned around the reactor. This thesis describes the dynamic safety analysis of the coupled neutron source, reactor core and reactor heat removal systems.

A special purpose simulation model was written to predict steady-state conditions and accident scenarios in SABR by calculating the coupled evolution of the power output from the fusion and fission cores and the axial and radial temperature distributions of a fuel pin in the reactor. Reactivity Feedback was modeled for Doppler and sodium coolant voiding. SABR has a positive temperature reactivity feedback coefficient. A series of accident scenarios were simulated to determine how much time exists to implement corrective measures during an accident before damage to the reactor occurs.

# CHAPTER I

# INTRODUCTION

With the increasing amount of spent nuclear fuel (SNF) and the soon to be growing fleet of nuclear reactors in the United States, closing the nuclear fuel cycle has become the next major technical challenge for the nuclear energy industry. By separating the transuranics (TRU) from the SNF discharged by Light Water Reactors (LWR), it is possible to fuel Advanced Burner Reactors (ABR) while minimizing the amount of SNF that must be stored in High Level Waste Repositories (HLWR) such as Yucca Mountain, where storage space will quickly become an issue. Fast Reactors being researched by the Generation IV Initiative (GEN-IV) will be capable of transmuting transuranics such as Plutonium, Americium and Neptunium. The Department of Energy's Global Nuclear Energy Partnership (GNEP) is developing Fuel Treatment Centers to separate these transuranics, which can then fuel ABRs.

With commercial nuclear power plants in the United States producing approximately 2,000 Metric Tons of SNF each year and already 56,000 MT of SNF produced over the past 5 decades [4], Yucca Mountain's legislative limit of 70,000 MT of SNF will be reached in less than 10 years. If the engineering limit of 120,000 MT of SNF is used instead, we would have less than 25 years before another repository is needed. Thirty-four new nuclear power plant applications are expected between 2007 and 2010, according to the Nuclear Regulatory Commission [2], which would increase nuclear power production by more than 30%. If we continue to use a once through cycle, we would need a new HLWR filled to its engineering limit every 40 years.

Investigations in the 1990s led to the conclusion that, instead of the current once through cycle, repeated reprocessing and recycling of fuel and the remaining transuranics could reduce waste that is sent to Waste Repositories by up to 90% [20, 1]. While in critical reactors a multiplication factor of 1 must be maintained, in subcritical reactors continued

exposure to neutrons will lead to arbitrarily high levels of burn-up regardless of the neutron multiplication level; but practical issues still remain such as material radiation damage. By achieving such deep burns, the quantity of high level waste required to be stored in repositories is greatly reduced.

One such subcritical reactor is the Subcritical Advanced Burner Reactor (SABR) being developed at the Georgia Institute of Technology [20]. SABR is a sodium-cooled fusion-driven reactor capable of burning TRU up to 25% over an 8.2 year residence time. The amount of TRU burned in SABR is limited by the radiation damage accumulation in the structural and cladding materials, but with repeated reprocessing and refrabrication, more than 90% of the TRU could be burned. SABR's tokamak D-T fusion neutron source is based on the International Thermonuclear Experimental Reactor (ITER) [3], which will begin operation in 2016 or 2017, and is capable of producing up to 500 MW of power. Since ITER will serve as a prototype for the SABR neutron source, SABR is being proposed as a second generation Advanced Burner Reactor.

A pure TRU-fueled reactor has a smaller delayed neutron fraction than light water reactors, which have large delayed neutron contributions from $^{235}$U; SABR's delayed neutron fraction is less than half of the $^{235}$U delayed neutron fraction. Fortunately, for SABR there is an extra level of safety due to the large margin to prompt criticality that comes with the reactor being subcritical. Because achieving supercriticality is nearly impossible in SABR the danger of operating with a small delayed neutron fraction is lessened. However, a small delayed neutron fraction does make the reactor more sensitive to reactivity feedbacks. The lack of uranium, specifically $^{238}$U, also leads to a worse Doppler reactivity feedback during reactor transients, but this too is partially mitigated by operating subcritically.

The purpose of this thesis is to examine what level of safety exists in SABR such that during a transient one would know how much time there is to implement corrective measures before irreparable damage to the reactor has occurred. This thesis examines the dynamics of the coupled fusion neutron source, fission core and heat removal systems.

# CHAPTER II

# SABR OVERVIEW

## *2.1 Configuration and Dimensions*

The Subcritical Advanced Burner Reactor is a sodium-cooled, metal-fueled, fast transmutation reactor with a tokamak D-T fusion neutron source. A simplified, three-dimensional view of the design is shown in Figure 1. Outside the tokamak fusion core is the 62-cm thick annular fission region and both the fusion and fission core are surrounded by a reflector, tritium-bleeding blanket and shield. The combined thickness of the reflector, breeding blanket and shield is 80 cm. Figure 1 does not include the plasma's divertor system, sodium coolant pipes or control rod drives.

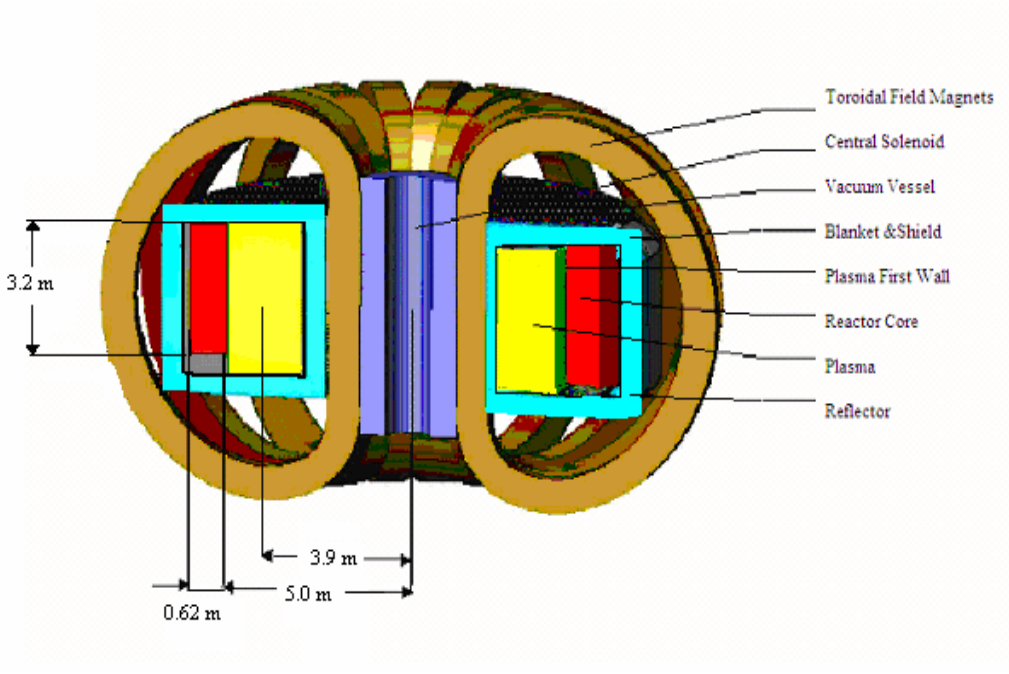


**Figure 1:** Configuration of SABR

In conjunction with the objectives of the GEN-IV initiative, SABR is designed to transmute the transuranics in SNF to reduce the waste loaded into high level waste repositories.

A secondary objective for SABR is the production of 3,000 MW of power which is then converted into electricity. To cool the reactor, a three loop cooling system with sodium in the intermediate loop and water in the secondary loop is utilized.

Figure 2 illustrates a simplified cross sectional view of the reactor with greater detail than Figure 1. The 3.2 m tall core is composed of 2 m of active fuel, a 1 m gas plenum and a 20 cm reflector capping the fuel rod. There are 918 hexagonal fuel assemblies, divided equally among the four fuel regions, each containing 271 fuel pins. Each fuel pin is 4 mm in diameter with transuranic/zirconium fuel and is clad in ODS steel. Sixteen of the 918 assemblies are enriched boron carbide control rods. These sixteen control rod assemblies will fit between each of the 16 magnets and provide roughly 9$ of negative reactivity.

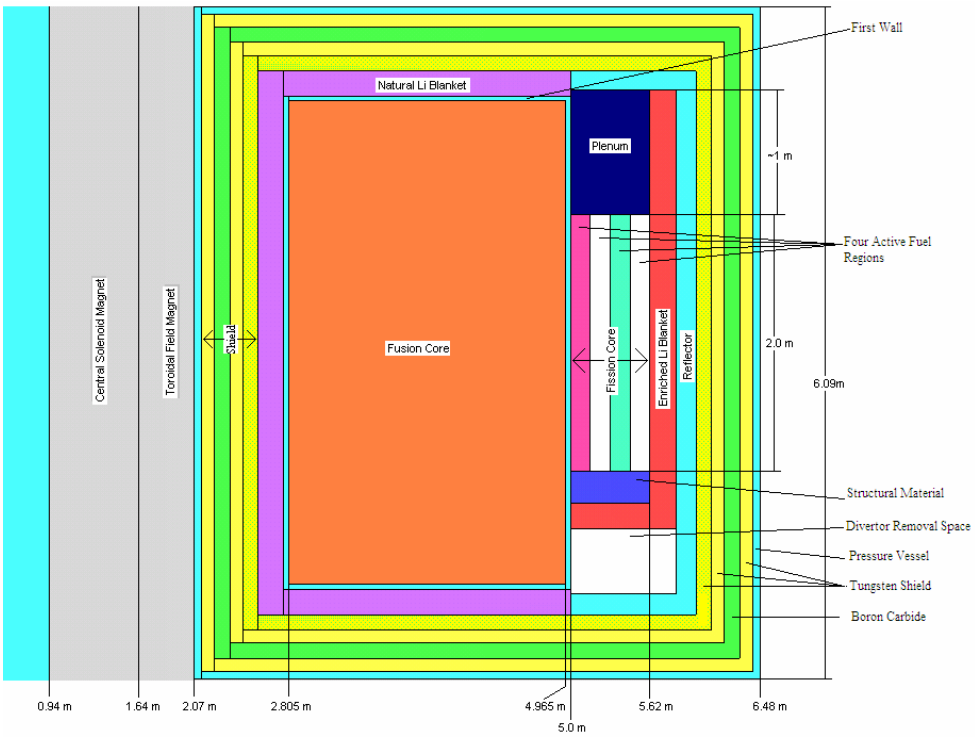


**Figure 2:** Cross Section of SABR

The fusion neutron source for SABR is the same source from the Gas-Cooled Fast Transmutation Reactor [20] developed at the Georgia Institute of Technology in 2006 and is a smaller version of the ITER design. The plasma's toroidal chamber is 3.76 m tall and

2.16 wide with a divertor (not shown in Figures 1 and 2) located at the bottom of the plasma chamber. In the region inside the plasma chamber is the superconducting solenoid magnet, which has an inner radius of 94 cm and an outer radius of 164 cm. Outside the shield region are sixteen D-shaped superconducting toroidal field magnets, which are 8.4 m in vertical bore and 5.4 m in horizontal bore with a radial thickness of 43 cm and toroidal thickness of 36 cm.

## *2.2 Major Parameters and Materials*

Table 1 gives a summary of the parameters associated with SABR. Table 2.2 lists the isotopic composition of the fuel at beginning of reactor lifetime (BOL), beginning of equilibrium cycle (BOC) and end of equilibrium cycle (EOC). BOL operation represents the time period just after the reactor is first turned on. BOC and EOC operation represent the initial and final states of the reactor in the equilibrium fuel cycle. Unless otherwise noted, all structural material is ODS (MA 957) steel.

## *2.3 TRU Fuel Element*

SABR utilizes metallic fuel which requires pyrometallurgic reprocessing. The fuel has a weight percent composition of 40Zr-10Am-10Np-40Pu. This fuel composition was chosen because of its high thermal conductivity, high fission gas retention and its ability to accommodate high actinide density [19, 15]. Extensive research at Argonne National Laboratory indicates metallic fuel as one of the frontrunners for transmutation reactors [19]. Zirconium is included in the fuel element to provide stability during irradiation, create a more negative Doppler feedback coefficient and also to increase the melting temperature of the alloy, which is 1,473 K. Table 3 gives the dimensions of the fuel rod while Figures 3 and 4 illustrate cross-sectional views of the fuel and one assembly, respectively. The melting temperature for the ODS cladding is 1,800 K and eutectic melting of the fuel and cladding occurs at 973 K.

**Table 1:** Major Parameters and Materials of SABR

| | |
|---|---|
| **Fission Core** | |
| Fission Power | 3,000 MWth |
| TRU Fuel Composition (w/o) | Pu-40, Am-10, Np-10, Zr-40 |
| Fuel Density | 9.595 g/cm$^3$ |
| Mass of TRU / Fuel Material | 36 MT / 60 MT |
| Specific Power | 83.3 kWth/kg TRU |
| Maximum $k_{eff}$ | 0.95 |
| Major Dimensions | $R_{in}$=5 m, $R_{out}$=5.62 m, $H_{active}$=2 m |
| Fuel Pin | #=248,778, $D_f$=4.00 mm, $D_o$=7.26 mm |
| Coolant Mass Flow Rate, Temperature | $\dot{m}$=8,700 kg/s, $T_{in}/T_{out}$=650/923 K |
| Power Density | $q'''$=72.5 MW/m$^3$ |
| Maximum Temperatures | $T_{f,max}$=969 K, $T_{clad,max}$=928 K |
| Linear Fuel Pin Power | 6 kW/ m |
| Clad, wire wrap and flow tube | ODS Ferritic Steel,<br>t=0.5 mm, 2.2 mm, 2.0 mm |
| Fuel/Clad, Gap, $LiNbO_3$<br>/Structure/Coolant (v/o) | <br>15/35/14/36 |
| Fuel Assembly | #=918, Hexagonal |
| **Reflector, Blanket and Shield** | |
| Reflector/Shield Materials | ODS Steel/$B_4C$, W, Na-cooled |
| Tritium Breeder | $Li_2SiO_4$ |
| Combined Thickness | 80 cm |
| Tritium Breeding Ratio | 1.16 |
| **Plasma** | |
| Plasma Current | 8.0 - 10.0 MA |
| Fusion Power | 50 - 500 MW |
| Neutron Source Rate | 1.8e19 s$^{-1}$ - 1.8e20 s$^{-1}$ |

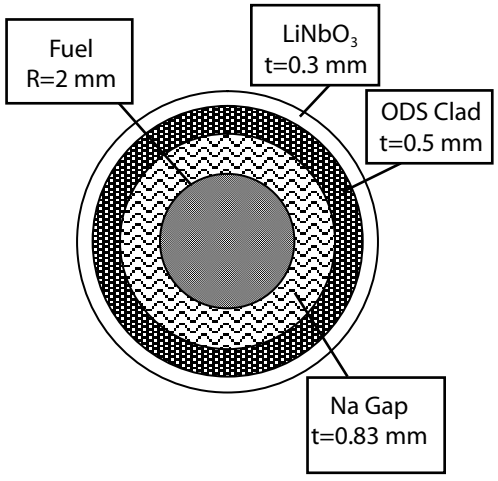


**Figure 3:** Cross-Sectional View of Fuel

**Table 2:** TRU Fuel Composition

| | Mass Percent | | |
|---|---|---|---|
| Isotope | BOL | BOC | EOC |
| $^{234}$U | 0.0 | 0.1 | 0.2 |
| $^{237}$Np | 17.0 | 15.8 | 14.9 |
| $^{238}$Pu | 1.4 | 4.3 | 6.7 |
| $^{239}$Pu | 38.8 | 35.1 | 32.4 |
| $^{240}$Pu | 17.3 | 19.1 | 20.4 |
| $^{241}$Pu | 6.5 | 5.7 | 5.1 |
| $^{242}$Pu | 2.6 | 3.2 | 3.7 |
| $^{241}$Am | 13.6 | 13.2 | 12.7 |
| $^{242m}$Am | 0.0 | 0.2 | 0.3 |
| $^{243}$Am | 2.8 | 2.7 | 2.7 |
| $^{242}$Cm | 0.0 | 0.2 | 0.3 |
| $^{244}$Cm | 0.0 | 0.3 | 0.5 |
| Other [a] | 0.0 | 0.1 | 0.1 |

[a]The remaining Fuel is composed of various Uranium, Plutonium and Curium Isotopes

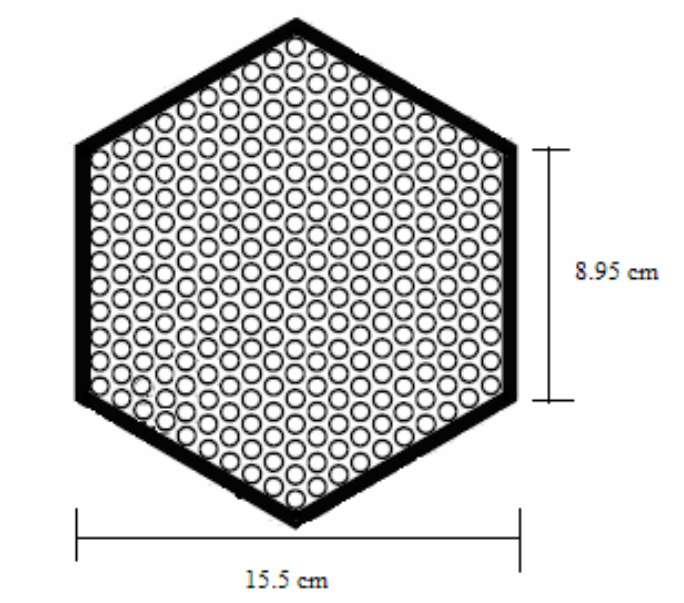


**Figure 4:** Cross-Sectional View of Assembly

### *2.4 Fusion Source Strength vs. Multiplication Constant*

While SABR is designed to operate at 3,000 MWth, the multiplication constant will decrease over time, which necessitates increasing the neutron source strength to maintain a constant power level. Starting with the neutron diffusion equation, Equation 1, one can derive

**Table 3:** Key Design Parameters of Fuel Pin and Assembly

| | | | |
|---|---|---|---|
| Length of rods (m) | 3.2 | $\text{Volume}_{plenum}/\text{Volume}_{fm}$ | 1.0 |
| Length of Fuel Material (m) | 2.0 | Total Pins in Core | 248,778 |
| Length of Plenum (m) | 1.0 | Pitch (mm) | 9.41 |
| Length of Reflector (m) | 0.2 | Pitch-to-Diamter Ratio | 1.3 |
| Radius of Fuel Material (mm) | 2.0 | Total Assemblies | 918 |
| Thickness of Clad (mm) | 0.5 | Pins per Assembly | 271 |
| Thickness of Na Gap (mm) | 0.83 | Flow Tube Thickness (mm) | 2 |
| Thickness of $LiNbO_3$ (mm) | 0.3 | Wire Wrap Diameter (mm) | 2.24 |
| Mass of Fuel Material/rod (g) | 241 | Coolant Area/Assembly ($cm^2$) | 75 |

a relationship between the required fusion neutron source strength as a function of the intended fission power and neutron multiplication level from the neutron balance.

$$\int_V \left[\vec{\nabla} \cdot D\vec{\nabla}\phi - \Sigma_a\phi + \nu\Sigma_f\phi\right] dV = -\int_V SdV \tag{1}$$

Using the divergence theorem on the streaming term and substituting $J$ in for $-D\vec{\nabla}\phi$ leads to Equation 2 where the subscripts $S$ and $V$ refer to the surface and volume of the system.

$$-\int_S \vec{J}\cdot\hat{n}dS - \int_V \Sigma_a\phi dV + \int_V \nu\Sigma_f\phi dV = -\int_V SdV \tag{2}$$

Equations 3 and 4 can then be substituted into Equation 2 to get Equation 5. $P_{fission}$ and $P_{fusion}$ represent the fission and fusion power levels while $E_{fission}$ and $E_{fusion}$ represent the average energy released per fission and fusion event.

$$P_{fission} = \frac{1}{\nu}E_{fission}\int_V \nu\Sigma_f\phi dV \Rightarrow \int_V \nu\Sigma_f\phi dV = \nu\frac{P_{fission}}{E_{fission}} \tag{3}$$

$$P_{fusion} = E_{fusion}\int_V SdV \Rightarrow \int_V SdV = \frac{P_{fusion}}{E_{fusion}} \tag{4}$$

$$-\int_S \vec{J}\cdot\hat{n}dS - \int_V \Sigma_a\phi dV + \nu\frac{P_{fission}}{E_{fission}} = -\frac{P_{fusion}}{E_{fusion}} \tag{5}$$

Rearranging the terms on the left side of Equation 5 leads to Equation 6:

$$\left[\frac{-\left(\int_S \vec{J}\cdot\hat{n}dS + \int_V \Sigma_a\phi dV\right)}{\int_V \nu\Sigma_f\phi dV} + 1\right] + \nu\frac{P_{fission}}{E_{fission}} = -\frac{P_{fusion}}{E_{fusion}} \tag{6}$$

Defining $k_m$ as:

$$k_m = \frac{\int_V \nu\Sigma_f\phi dV}{-\left(\int_S \vec{J}\cdot\hat{n}dS + \int_V \Sigma_a\phi dV\right)} = \ldots$$

$$\ldots = \frac{\text{Fission Neutron Production}}{\text{Total Neutron Leakage + Neutron Absorption}} \tag{7}$$

leads to Equations 8:

$$\frac{1-k_m}{k_m}\nu\frac{P_{fission}}{E_{fission}} = -\frac{P_{fusion}}{E_{fusion}} \tag{8}$$

Equation 8 can then be rearranged to give Equation 9, which gives the required fusion power level as a function of the desired fission power and neutron multiplication level, $k_m$.

$$P_{fusion} = \frac{E_{fusion}}{E_{fission}}\nu\frac{1-k_m}{k_m}P_{fission} \tag{9}$$

Table 4 lists the required fusion power level as well as the neutron multiplication level for various stages of reactor operation. For D-T fusion and actinide fission, $E_{fus}$ = 17.6 MeV and $E_{fis}$ = 197 MeV, while $\nu$ was calculated to be 2.98 from the Monte Carlo code MCNP [10, 20]. The neutron multiplication level, $k_m$ was calculated as defined in Equation 7 by fission and absorption reaction tallies in MCNP over the volume of the system as well as leakage tallies over SABR's outermost surface. The effect of (n,2n) and (n,3n) reactions on $k_m$ was minimal.

To sustain 3,000 MW of fission power at BOL with $k_m$ = 0.878, 111 MW of fusion power are required. If SABR's neutron source were to operate at the full design capacity of 500 MW, the multiplication constant could drop as low as 0.6 and the full power of 3000 MW could be maintained. To achieve the operational parameters necessary for SABR, the fusion neutron source requires an external heating and current drive (H&CD) system. An H&CD system consisting of six lower hybrid (LH) wave launchers was chosen with each wave launcher providing approximately 20 MW of heating and 1.5 MA of current drive [9].

**Table 4:** Required Fusion Neutron Source Strength vs. TRU Fuel Cycle

| | BOL | BOC | EOC |
|---|---|---|---|
| $k_{eff}$ | 0.95 | 0.88 | 0.83 |
| $k_m$ | 0.88 | 0.81 | 0.79 |
| Required $P_{fus}$ (MW) | 111 | 183 | 218 |

### *2.5 Heat Removal System*

SABR utilizes a three loop core heat removal system. Liquid sodium in the primary loop removes the core's heat, which is transferred to an intermediate loop, also with liquid

sodium. Heat in the intermediate loop converts water in the secondary loop to steam which passes through turbines generating electricity. Thermal properties of the fuel, clad and coolant are given in Table 5. The coolant mass flow rate through the core is 8,695 kg/s through a total flow area of 7.5 $m^2$. At steady state, the coolant inlet temperature to the core is 650 K and the outlet temperature is 923 K.

**Table 5:** Thermal Properties of Fuel Pin and Coolant at Steady State Operation

| | |
|---|---|
| Conductivity of Sodium ($k_{Na}$) | 6.26E-05 MW/m · K |
| Specific Heat Capacity ($c_p$) | 1.27 kJ/kg · K |
| Heat Transfer Coefficient ($h_{Na}$) | 0.05731 MW/$m^2$ · K |
| Sodium Viscosity ($\mu_{Na}$) | 2.28E-04 |
| Pitch to Diameter (P/D) | 1.3 |
| Conductivity of Cladding ($k_c$) | 3.0E-05 MW/m · K |
| Conductivity of Fuel ($k_f$) | 1.0E-05 MW/m · K |
| Conductivity of Gap ($k_g$) | 5.0E-04 MW/m · K |
| Conductivity of Coolant ($k_{Na}$) | 6.26E-05 MW/m · K |
| Outer Clad Radius | 0.0033 m |
| Inner Clad Radius | 0.0028 m |
| Fuel Radius | 0.002 m |
| Flow Area of Core | 7.5 $m^2$ |
| Pump Efficiency ($\eta$) | 0.85 |
| Density of Sodium ($\rho$) | 829 kg/$m^3$ |
| Reynolds Number | 31,525 |
| Peclet Number | 145 |
| Equivalent Hydraulic Diameter | 6.2 mm |

### *2.6 Transmutation and Electrical Performance*

SABR is able to transmute 1.06 MT of transuranics every effective full power year. For the 100,000 MWe of power produced each year, nuclear reactors produce 2,000 MT of spent nuclear fuel per year [7] of which 1% is transuranics or approximately 0.2 MT/year of transuranics from one average 1,000 MWe Light Water Reactor. If run at 100% capacity, SABR would be able to burn the annual transuranic discharge from five 1,000 MWe LWRs [20].

The 3,000 MW of thermal power produced in SABR's fission core is converted to 1,049 MWe by the turbine. Of this 1,049 MWe, less than 100 MWe will be used to power the fusion neutron source, while the pumps will use 7.7 MWe and the heaters 30 MWe. With

a net electrical power 911 MWe, SABR has a net efficiency of 30.4%. Because SABR was not designed with power production efficiency as the primary objection, there is room to improve on this number.

# CHAPTER III

# DYNAMICS CALCULATIONAL MODEL

Transients develop differently for critical and subcritical systems. In a critical system, an introduction of reactivity will lead to a prompt jump of the fission power followed by a gradual increase or decrease due to the decayed neutrons. For derivates of the neutron kinetics equations, Equations 25 and 26 in Section 3.2, greater than zero, the neutron population will increase monotonously. For positive reactivity insertions, the reactor will become supercritical while for negative reactivity insertions, the reactor will shut itself down. Control rods and negative reactivity feedbacks, however, allow for new steady-state power levels and temperatures to be achieved and criticality reestablished.

Subcritical systems, which require an external source of neutrons to maintain steady-state operation, respond differently to reactivity insertions in that the reactor will always reach a new steady-state after the reactivity insertion, even without control rods or reactivity feedback. As long as criticality is not achieved, the reactor will reach a new equilibrium.

The Transient Analysis Program for Accidents in SABR (TAPAS) is a simplified model special purpose code written to calculate the power levels and temperatures in the reactor. TAPAS simulates dynamics conditions and accident scenarios in SABR by coupling the three major systems in the reactor: the fusion neutron source, the fission core and the heat removal systems. The fusion and fission systems are modeled as point models, i.e. there is no spatial dependence on the power levels. The heat removal system calculates the axial and radial temperature distributions of one representative fuel pin. In order to simulate accident scenarios, one or more parameters, such as coolant velocity, are instantaneously or gradually changed to a new value. Two criteria are used to determine if the reactor has sustained permanent damage: coolant boiling and fuel melting. The melting temperature for the ODS cladding is 1,800 K and eutectic melting of the fuel and cladding occurs at 973 K. Cladding creep will become an issue at temperatures much lower than the melting

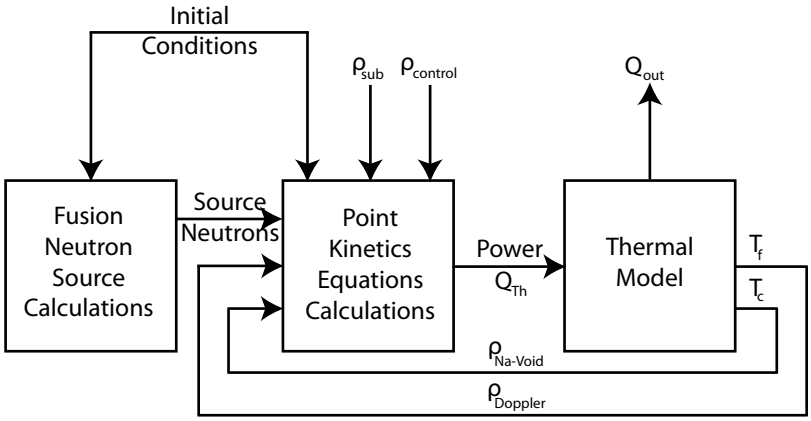


**Figure 5:** TAPAS Program Flow Chart

temperature and for similar ODS steels this temperature is around 1,500 K. The temperature at which creep becomes an issue for MA 957 is still being investigated as it is a relatively new alloy, however, the melting temperature of SABR's fuel is lower than 1,500 K and thus the fuel will fail first. It should also be noted that creep is only an issue over longer time scales than those investigated in this study. Because damage to the core due to eutectic melting between the cladding and the fuel is not well understood, the eutectic limit is not considered as a constraint in the accident scenarios.

### *3.1 Fusion Neutron Source*

The governing equations for a D-T fusion neutron reaction are an energy balance over the plasma internal energy, U, between the heating sources and the power losses [17] and the particle balance equations for the ions, alpha particles and impurities in the plasma. The heating sources in Equation 10 are $P_\alpha$, which is the energy released during a fusion event in the form of a 3.5 MeV alpha particle, and $P_{aux}$, which is the auxiliary power used to heat the plasma. The energy loss terms, $P_{Rad}$ and $P_{Tr}$, are the power losses due to radiation and transport, respectively.

$$\frac{dU}{dt} = (P_\alpha + P_{aux}) - (P_{Rad} + P_{Tr}) \tag{10}$$

The auxiliary heating to the plasma in SABR comes from six 20 MW lower hybrid

electromagnetic wave launchers [9]. The alpha heating term is governed by Equation 11 where $n_i = n_D + n_T$ is the ion density, $U_\alpha$ is the 3.5 MeV alpha energy deposited in the plasma for each fusion event and $\langle < \sigma \cdot v > \rangle_f$ is the fusion reaction rate.

$$P_\alpha = \frac{1}{4} n_i^2 \langle \sigma \cdot v \rangle_f U_\alpha \tag{11}$$

The loss term due to radiation is composed of a bremsstrahlung term and an impurity radiation term, shown in Equations 12-14. The transport power loss is given in Equation 15 [17].

$$P_{Rad} = P_{brem} + P_{imp} \tag{12}$$

$$P_{brem} = 1.7 \times 10^{-38} n_i n_e T^{0.5} \sum_{j=z} \frac{n_j z_j^2}{n_e} \tag{13}$$

$$P_{imp} = (1 + 0.3T) \times 10^{-43} n_e n_z z^{3.7 - 0.33 lnT} \tag{14}$$

$$P_{Tr} = \frac{U}{\tau_E} = \frac{3 n_i T}{\tau_E} \tag{15}$$

In the above equations, $n_i$, $n_e$ and $n_z$ are the ion, electron and impurity densities in the plasma, respectively, and are assumed to have a Maxwellian velocity distribution and the same average temperature, $T$, in the plasma. The ion and electron densities were assumed to be the same and are governed by Equation 16, where $S_i$ represents the external source of ions and $\tau_E$ is the confinement time.

The governing equations for the alpha particle and impurity ion densities are given in Equations 17-18, where $S_\alpha$ and $S_z$ represent external sources of alpha particles and impurity ions including recycling and sputtering from the first wall and external fueling. A simple assumption for the impurities represented the impurity densities as a fraction of the ion density. Upper limits for normal operation are placed on the impurity densities at 0.025% and 5% for tungsten and carbon, respectively. Impurity radiation was calculated for carbon, tungsten and alpha particles. The decision to use tungsten and carbon for the impurity calculations comes from the present design for ITER, which serves as the design basis for SABR's neutron source. ITER currently incorporates tungsten divertor target plates and there is consideration of using a carbon coating for the steel walls. With approximately

one-fifth of the energy of each fusion event going into the alpha particle and the remaining energy into the neutron, the fusion power level is five times the alpha power.

$$\frac{dn_i}{dt} = S_i - \frac{1}{2} n_i^2 \langle \sigma \cdot v \rangle_f - \frac{n_i}{\tau_P} \tag{16}$$

$$\frac{dn_a}{dt} = S_a + \frac{1}{4} n_i^2 \langle \sigma \cdot v \rangle_f - \frac{n_a}{\tau_P} \tag{17}$$

$$\frac{dn_z}{dt} = S_z - \frac{n_z}{\tau_P} \tag{18}$$

where $\tau_P$ is the particle confinement time. This value is hard to measure and is assumed to be approximately the same as the energy confinement time, $\tau_E$.

The correlation used to calculate the H-Mode Energy Confinement time, $\tau_E$, is given by:

$$\tau_E = 0.144\ h\ \frac{I^{0.93} B^{0.15} (n_i/10^{20})^{0.41} M^{-0.58} R^{1.97} \kappa^{0.78}}{(P_{aux} + P_\alpha)^{0.69}} \tag{19}$$

where $I$ is the plasma current, $B$ is the toroidal magnetic field, $M$ is the molecular mass of the plasma ions, $R$ is the major plasma radius, $\kappa$ is the plasma elongation and $P$ is heating power, $P_\alpha$ and $P_{aux}$. For our D-T plasma, $M$ is 2.5, $I$ is 9 MA, $\kappa$ is 1.7, $R$ is 3.75 m and $B$ is 11.8 Tesla. This correlation was developed from measured energy confinement times from tokamak experiments in the high confinement regimes [17]. The above parameters for SABR's fusion neutron source are within the design basis for ITER and have already been achieved. In Equation 19, the variable $h$ represents anticipated improvements in energy confinement.

The operating parameters used in SABR for the fusion neutron source are given in Table 3.1. There are three levels at which the fusion reactor operates in the SABR simulations: beginning of reactor lifetime (BOL), beginning of equilibrium cycle (BOC) and end of equilibrium cycle (EOC).

In Table 3.1, the fusion reaction rate, $\langle < \sigma \cdot v > \rangle_f$, for the D-T plasma is calculated using a correlation [5] shown below that was developed by Bosch and Hale in the early 1990s to better fit experimental data. $\theta$ and $\zeta$, in Equations 20-22, are parameter fits for the correlation and are applicable over temperatures from 0.2-100 keV.

$$\theta = \frac{T}{1 - \frac{T(0.01514 + T(0.004606 - 1.0675 \times 10^{-4} \times T))}{1 + T(0.07519 + T(0.0135 + 1.366 \times 10^{-5} \times T))}} \tag{20}$$

**Table 6:** Plasma Operating Parameters

| | BOL | BOC | EOC |
|---|---|---|---|
| $P_{fus}$ (MW) | 111 | 183 | 218 |
| $n_i$ ($m^3$) | 8.80E19 | 8.54E19 | 8.80E19 |
| T (keV) | 13.89 | 19.37 | 21.14 |
| $P_{aux}$ (MW) | 40 | 60 | 80 |
| $\tau_{aux}$ (s) | 0.98 | 0.78 | 0.67 |
| $\langle \sigma \cdot v \rangle_f$ ($m^3$/s) | 2.37E-22 | 4.14E-22 | 4.66E-22 |
| % of $\beta$-Limit | 0.80 | 0.98 | 0.98 [a] |
| I (MA) | 9.02 | 9.9 | 10.00 |
| $Q_p$ | 2.78 | 3.05 | 2.73 |

[a]Plasma Operation during EOC is using a $\beta_N$ of 2.8, which is discussed below

$$\varsigma = \left( \frac{1182.17}{4\theta} \right)^{1/3} \tag{21}$$

$$\langle \sigma \cdot v \rangle_f = 1.173 \times 10^{-15} \times \theta \times \left( \frac{\varsigma}{1,124,656\ T^3} \right)^{0.5} e^{-3\varsigma} \tag{22}$$

The operation of the plasma with respect to the Troyon Beta Limit, which is discussed below, is given as a percentage of the maximum allowable value of the product of the ion density and temperature in the plasma. Finally, $Q_p$ is the ratio of total fusion power to the external heating power. With all elements of Equation 10 known, the fusion power can be found for the desired level of neutron multiplication.

There are three primary mechanisms for controlling or shutting down the plasma:

- adjusting the plasma auxiliary heating,
- adjusting the ion fueling rate and,
- impurity injection to increase the impurity density.

At normal operation, the auxiliary heating source to the plasma is at 40, 60 or 80 MW and decreasing this value effectively shuts down the plasma. This decrease in fusion power occurs on the same time scale as the energy confinement time, which is less than one second, for an instantaneous drop in auxiliary heating. With an ion confinement time on the order of a few seconds, it is necessary to constantly fuel the plasma to keep the fusion power level constant. If this fueling rate is decreased, the power in the reactor also decreases.

Finally, increasing the impurity density in the plasma by impurity injection will increase the radiation power loss and thus decrease the fusion power. The time scale for changes in the fusion power level due to ion fueling rate or impurity density adjustments is a function of how long it takes for the ions and impurities to vacate their respective injection tubes, usually a few seconds. An accidental increase in the auxiliary heating or ion fueling rates will be analyzed later to determine its effects on SABR.

During operation of the plasma, there are two limits that prevent the plasma ion density from growing too large: the Troyon Beta and Greenwald Density Limits. As either limit is approached, the energy confinement time begins to deteriorate, gradually at first but more significantly as the plasma operating parameters get closer to the limits. These density limits act as a small negative feedback during power excursions to reduce fusion power increases

The Troyon Beta limit, which provides an upper limit on both the plasma temperature and ion density beyond which plasma stability and confinement are lost, is given below [17]:

$$\frac{2n_i kT}{B(T)^2/2\mu_0} \leq \beta_N \frac{I(MA)}{a(m) \cdot B(T)} \tag{23}$$

where $B$ is the magnetic field strength, $I$ is the current and $a$ is the minor radius. For present experiments $\beta_N$ varies between 2.5-3.0, although many experiments operate stably at higher values. Increasing the stable value of $\beta_N$ is an objective of present fusion research. Accommodating higher values of $\beta_N$ is possible by optimizing the current profile in the plasma. With the parameters listed above in Table 6 for BOL and BOC operation, SABR would have a $\beta_N$ of 2.5 while during EOC operation, SABR would have a $\beta_N$ of 2.8. The effect of the Troyon Beta Limit during fusion related transients is examined in more detail in Section 4.

The Greenwald Density Limit, given in Equation 24, is a simple empirical fit that bounds the densities for tokamak plasmas [17]. The Greenwald Density Limit, which is much higher than the normal plasma operating density by about 150%, is not reached during any of the accidents simulated in this thesis.

$$n_G = I/\pi a^2 \tag{24}$$

### *3.2 Neutron Kinetics*

The neutron population in the reactor is calculated using the neutron kinetics equations given in Equations 25 & 26 for the neutron precursor population, $C_j$, and neutron population, $n$:

$$\frac{dC_j}{dt} = \frac{\beta_j}{\Lambda} n - \lambda_j C_j \tag{25}$$

$$\frac{dn}{dt} = \frac{\rho_{tot} - \beta}{\Lambda} n + \sum_j \lambda_j C_j + S \tag{26}$$

where $\Lambda$ is the neutron lifetime, and $\lambda_j$ and $\beta_j$ are the decay constants and delayed neutron fractions for each of the six delayed neutron groups, respectively [16]. $\beta$ is the total delayed neutron fraction. The fusion neutron source is taken into account by $S$, which is the number of D-T neutrons that reach the fission core. The total reactivity, $\rho_{tot}$, is defined by:

$$\rho_{tot} = \rho_{sub} + \rho_{Doppler} + \rho_{Na-void} + \rho_{ex} \tag{27}$$

where $\rho_{sub}$ is $(k_{eff} - 1)/k_{eff}$, $\rho_{Doppler}$ is the reactivity feedback due to Doppler broadening, $\rho_{Na-void}$ is the reactivity feedback due to sodium voiding and $\rho_{ex}$ accounts for external reactivity insertions such as control rod withdrawals. The reactivity feedbacks due to Doppler broadening and sodium voiding are discussed later. Using the total delayed neutron fraction of $\beta = 0.003$ for the TRU fuel, it was calculated that during BOL operation SABR is operating at $\rho'_{sub}$ = -17.5\$, where $\rho' = \frac{\rho}{\beta}$. Equations 25 & 26 can be combined to give the steady-state neutron population as a function of the total reactivity and source strength:

$$n = \frac{-S \cdot \Lambda}{\rho_{tot}} \tag{28}$$

In critical reactors the typical way to counteract inadvertent positive reactivity insertions is through the addition of negative reactivity from control rod insertion. Control rod insertion will produce an immediate prompt jump decrease in the neutron level followed by a slow decrease on the delayed neutron timescale. However, in a subcritical reactor, due to the constant source of neutrons streaming from the plasma, a control rod insertion cannot force the power in the fission core to zero. Control rod insertions in subcritical reactors will lead to a reduction of the neutron and fission power levels to a new steady-state value.

A different way to control subcritical reactors is through reduction of the neutron source strength. Reductions in the neutron source strength will lead to neutron and fission power level decreases on the prompt neutron timescale. Further, turning off the neutron source will lead to a nearly instantaneously reduction of the neutron and fission power to zero. Thus, while control rod insertion is the most effective control mechanism in critical reactors, a reduction or termination of the neutron source is the most effective control mechanism in subcritical reactors.

Delayed neutron fractions and decay constants for Equations 25 & 26 are readily available for more traditional nuclear fuels like plutonium and uranium. However, with americium and neptunium in our fuel, SABR's delayed neutron parameters cannot simply be looked up in a table. VAREX [11] was used to calculate the delayed neutron fractions and decay constants for the SABR fuel. VAREX uses data libraries containing delayed neutron production and energy distribution data based on the JEF2.2 nuclear data set to calculate the delayed neutron fractions and decay constants for each nuclide for a specified geometry. The mean neutron lifetime, $\Lambda$, was calculated using the discrete ordinates code XSDRN from the SCALE [13] code package by performing the flux weighted average of Equation 28:

$$\Lambda = \frac{\sum_j \lambda_j C_j}{\sum_g v_g \cdot (\nu \cdot \Sigma_f)_g \cdot \phi_g} \tag{29}$$

The mean neutron lifetime was found to be $1.7 \cdot 10^{-7}$ seconds, which is consistent for fast reactors and considerably shorter than for thermal reactors [16]. The XSDRN pin-cell calculations used ENDF/B-VI cross sections that were collapsed from 238 groups to 27 groups using SCALE's Control Module for Enhanced Criticality Safety Analysis Sequences (CSAS).

Reactivity feedbacks for Doppler and sodium voiding were calculated as functions of temperature changes such that:

$$\alpha_{Doppler} = \frac{\Delta\rho}{\Delta T_{fuel}} \tag{30}$$

$$\alpha_{Na-void} = \frac{\Delta\rho}{\Delta T_{coolant}} \tag{31}$$

The reactivity feedback from Doppler was calculated using VAREX to be $\alpha_{Doppler} = -2.20 \cdot$

**Table 7:** Delayed Neutron Parameters for Fresh Fuel and BOC and EOC Equilibrium Fuel

| Group | $\beta_i$ | $\lambda_i(1/s)$ |
|---|---|---|
| 1 | 8.308E-5 | 1.324E-2 |
| 2 | 7.623E-4 | 3.019E-2 |
| 3 | 5.836E-4 | 1.166E-1 |
| 4 | 1.059E-3 | 3.133E-1 |
| 5 | 4.139E-4 | 1.046 |
| 6 | 1.069E-4 | 2.837 |
| Total | 3.009E-3 | - |

$10^{-7}$ per Kelvin increase in the fuel temperature. The feedback due to sodium voiding was calculated to be $\alpha_{Na-void} = 2.06 \cdot 10^{-5}$ per Kelvin increase in the coolant temperature using a pin-cell calculation in XSDRN. The leakage component of sodium voiding is due to the reduction in sodium density with temperature increase. A lower coolant density leads to more neutrons leaking from the core and a decrease in reactivity. The non-leakage component of sodium voiding is due to the harder neutron spectrum resulting from the reduced coolant density. At higher energies, both the fission-to-capture ratio and average number of neutrons released per fission increase resulting in reactivity increasing.

### *3.3 Heat Removal*

Because the pipes leading into the heat exchanger were not designed and a fully time dependent thermal hydraulics model would require a much more powerful program, the heat exchanger is a quasi-time-independent model in TAPAS without any temporal delay between the coolant exiting and reentering the fission core. The equations used to solve for the axial temperature distributions in a fuel rod are quasi-steady-state. These equations are used because the thermal time constant [8], shown below in Equation 32, was calculated to be 0.025 seconds, or one-fourth of the time step used in the model. In Equation 32, the first term is the resistance to convective heat transfer. The second term is the lumped thermal capacitance of the fuel with the transfer coefficient of the fuel, $h_{fuel}$, equaling 57,300 $W/m^2 \cdot K$, the fuel density $\rho_{fuel}$ is 9,595 $kg/m^3$ and the fuel specific heat $c_p$ is 150 $J/kg \cdot K$. $V_{rod}$ is the volume of an individual fuel rod.

$$\tau = \left( \frac{1}{h_{fuel} \cdot A_s} \right) (\rho_{fuel} \cdot V_{rod} \cdot c_p) \tag{32}$$

The axial fuel pin power profile was approximated as a sinusoidal distribution with a peaking factor of 1.4, as seen in Figure 6 where the horizontal bars represent the top and bottom of the active fuel rod. The effect of using different peaking factors is discussed in Section 4.4. Equation 33 can be solved for the extrapolation length, $L_e$, of the flux profile, which represents the distance over which the flux profile would go to zero in a bare fuel rod. For a peaking factor of 1.4, the extrapolation length is 2.29 m and the peak linear heat-generation rate, $q_0$ is 8,441 W/m, which does not take radial power peaking into account.

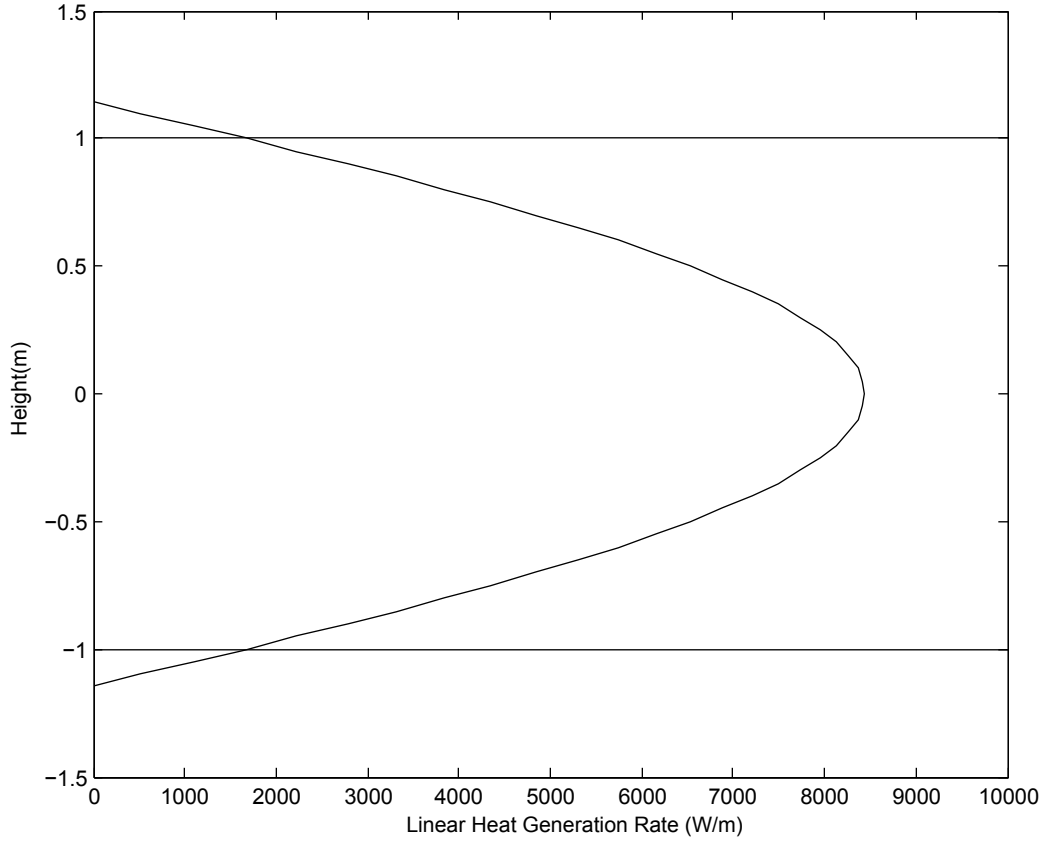


**Figure 6:** Axial Power Distribution for an Average Fuel Rod

$$q^{'}(z) = q_0^{'} cos\left[\frac{\pi \cdot z}{L_e}\right] \tag{33}$$

The axial temperature distributions for the coolant, outer and inner clad, fuel surface and fuel centerline given below in Equations 34-38 are found in Reference [18].

$$T_{coolant}(z) = T_{in} + q_0^{'}\left(\frac{L_e}{\pi \dot{m} c_p}\right)\left(sin\frac{\pi z}{L_e} + sin\frac{\pi L}{2L_e}\right) \tag{34}$$

$$T_{co}(z) = T_{in} + q_0^{'}\left(\frac{L_e}{\pi \dot{m} c_p}\left(sin\frac{\pi z}{L_e} + sin\frac{\pi L}{2L_e}\right) + \frac{1}{2\pi R_{co} h_c} cos\frac{\pi z}{L_e}\right) \tag{35}$$

$$T_{ci}(z) = T_{in} + q_0^{'}(\frac{L_e}{\pi \dot{m} c_p}\left(sin\frac{\pi z}{L_e} + sin\frac{\pi L}{2L_e}\right) + \ldots$$
$$\ldots + \left(\frac{1}{2\pi R_{co} h_c} + \frac{1}{2\pi k_c} ln\left(\frac{R_{co}}{R_{ci}}\right)\right) cos\frac{\pi z}{L_e}) \tag{36}$$

$$T_{fs}(z) = T_{in} + q_0^{'}(\frac{L_e}{\pi \dot{m} c_p}\left(sin\frac{\pi z}{L_e} + sin\frac{\pi L}{2L_e}\right) + \ldots$$
$$\ldots + \left(\frac{1}{2\pi R_{co} h_c} + \frac{1}{2\pi k_c} ln\left(\frac{R_{co}}{R_{ci}}\right) + \frac{1}{2\pi R_g h_g}\right) cos\frac{\pi z}{L_e}) \tag{37}$$

$$T_{cl}(z) = T_{in} + q_0^{'}(\frac{L_e}{\pi \dot{m} c_p}\left(sin\frac{\pi z}{L_e} + sin\frac{\pi L}{2L_e}\right) + \ldots$$
$$\ldots + \left(\frac{1}{2\pi R_{co} h_c} + \frac{1}{2\pi k_c} ln\left(\frac{R_{co}}{R_{ci}}\right) + \frac{1}{2\pi R_g h_g} + \frac{1}{4\pi k_f}\right) cos\frac{\pi z}{L_e}) \tag{38}$$

In the above equations, $T_{in}$ is the coolant inlet temperature, $k_c$ and $k_f$ are the cladding and fuel thermal conductivities, $h_c$ and $h_g$ are the coolant and gap heat transfer coefficients and $R_{co}$ and $R_{ci}$ are the outer and inner cladding radii. The various thermal conductivities in the fuel pin are given in Table 5 in Section 2.5. The correlations below to calculate the sodium heat transfer coefficient were also taken from reference [18].

$$h_{Na} = k_{Na} \cdot \frac{Nu}{D_e} \tag{39}$$

$$Nu = 4.0 + 0.33(P/D)^{3.8}(Pe/100)^{0.86} + 0.16(P/D)^{5.0} \tag{40}$$

$$Pe = Re \cdot Pr \tag{41}$$

$$Re = \frac{\dot{m} D_e}{\mu_{Na} \cdot A_f} \tag{42}$$

$$Pr = c_{p,Na}\frac{\mu_{Na}}{k_{Na}} \tag{43}$$

where $D_e$ is the equivalent hydraulic diameter, or $4A_f/P_w$, $P/D$ is the pitch-to-diameter ratio, $\mu_{Na}$ is the sodium viscosity, $A_f$ is the coolant flow area per pin, $P_w$ is the wetted perimeter and $c_{p,Na}$ is the specific heat of sodium. The equivalent hydraulic diamter for SABR's fuel pins is 6.2 mm. The correlation for $Nu$ given in Equation 40 is valid for

pitch-to-diameter ratios between 1.1 and 1.4 as well as Peclet numbers between 10 and 5,000.

Calculating the vertical position of the maximum temperature for the coolant, cladding and fuel requires setting the derivatives of Equations 34, 36 & 38 equal to zero, as shown in Equations 44-46. The coolant's maximum temperature will always be located at the outlet of the core. As the axial power profile becomes flatter, the location of the maximum cladding temperature will be closer to the outlet of the core. The maximum fuel centerline and surface temperatures occur close to the center of the fuel rod. For maximum temperature locations that occur outside the active fuel region, the outlet position of the core is used instead.

$$z_{cool} = \frac{\pi}{2}\frac{L_e}{\pi} \tag{44}$$

$$z_{clad} = \frac{L_e}{\pi} tan^{-1}\left[\frac{L_e}{\pi \dot{m} c_{p,Na}}\left(\frac{1}{2\pi R_{co} h_c} + ln\left(\frac{R_{co}}{R_{ci}}\right)\frac{1}{2\pi k_c}\right)^{-1}\right] \tag{45}$$

$$z_{fuel} = \frac{L_e}{\pi} tan^{-1}\left[\frac{L_e}{\pi \dot{m} c_{p,Na}}\left(\frac{1}{2\pi R_{co} h_c} + ln\left(\frac{R_{co}}{R_{ci}}\right)\frac{1}{2\pi k_c} + \frac{1}{2\pi R_g h_g} + \frac{1}{4\pi k_f}\right)^{-1}\right] \tag{46}$$

After calculating the axial temperature profiles in the fuel pin, coolant at the outlet temperature is fed into the counter flow heat exchanger. The intermediate loop consists of sodium at an inlet temperature of 590 K. At steady-state, the temperature of the sodium on the primary side is 60 K higher than the sodium on the intermediate side of the heat exchanger. A simple model of the heat exchanger was used to calculate the heat removal and thus the new coolant inlet temperature to the core [8]:

$$Q_{out} = h \cdot A \frac{\Delta T_1 - \Delta T_2}{ln(\Delta T_1 / \Delta T_2)} = C_0 \frac{\Delta T_1 - \Delta T_2}{ln(\Delta T_1 / \Delta T_2)} \tag{47}$$

where $\Delta T_1$ is the temperature difference across the heat exchanger between the primary and intermediate sodium at the hottest part of the heat exchanger, while $\Delta T_2$ is the temperature difference at the coldest part of the heat exchanger. $C_0$ represents the overall heat transfer coefficient of the heat exchanger. For fluids with the same heat capacity rates, or $\dot{m}c_p$, the right side of Equation 47 can be replaced by $h \cdot A \cdot \Delta T_1$; this occurs at steady-state in SABR.

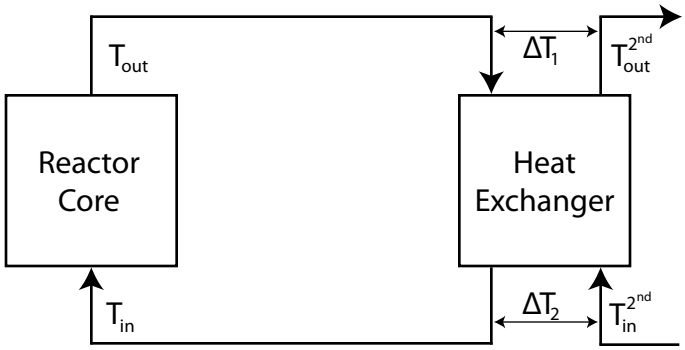


**Figure 7:** Calculational Model of SABR's Heat Exchanger

### *3.4 Coupling of the Systems*

To accurately model the power level and temperatures at discrete time steps in SABR, the three major systems described above - the fusion neutron source, neutron kinetics and heat removal - are coupled together in TAPAS. The fusion system calculates the number of source neutrons that reach the fission core and then the neutron kinetics system calculates the power level in the reactor. The fission power level is fed into the thermal system which calculates the radial and axial temperature distributions in a fuel pin and also the heat removed by the heat exchanger. Finally, the reactivity feedbacks are calculated based on the temperature changes in the fuel and coolant.

The first calculations TAPAS performs are a determination of the plasma confinement time and the fusion reaction rate, Equations 19-22. Next, the power gains and loss terms in the plasma are calculated from Equations 11-14. With this information, Equation 10 is discretized with respect to time to solve for the new plasma internal energy, which then allows for the new plasma temperature to be calculated. Finally the fusion power is calculated and thus the number of source neutrons streaming into the fission core is known.

By discretizing Equation 25 in time, it is possible to solve for the number of precursors at each subsequent time step. Equation 25 then becomes Equation 48, below. Because the neutron population changes on a very short time scale, less than $10^{-6}$ seconds, and the

neutron population is being calculated every tenth of a second, the left side of Equation 26 can be set to zero to give Equation 49. This is the prompt jump approximation:

$$C_j\left[t_{i+1}\right] = C_j\left[t_i\right] + dt\left(\frac{\beta_j}{\Lambda} n\left[t_i\right] - \lambda_j C_j\left[t_i\right]\right) \tag{48}$$

$$n\left[t_{i+1}\right] = \frac{\Lambda}{\beta - \rho_{tot}\left[t_i\right]}\left(\sum_j \lambda_j C_j\left[t_{i+1}\right] + S\left[t_{i+1}\right]\right) \tag{49}$$

Equations 48 and 49 can be modified to account for the fission power level in the core to become:

$$C_j^{'}\left[t_{i+1}\right] = C_j^{'}\left[t_i\right] + dt\left(\frac{\beta_j}{\Lambda} P\left[t_i\right] - \lambda_j C_j^{'}\left[t_i\right]\right) \tag{50}$$

$$P\left[t_{i+1}\right] = \frac{\Lambda}{\beta - \rho_{tot}\left[t_i\right]}\left(\sum_j \lambda_j C_j^{'}\left[t_{i+1}\right] + S^{'}\left[t_{i+1}\right]\right) \tag{51}$$

The power level $P$ scales to the neutron population as:

$$P = \int_V \int_E v\left(E\right) n\left(r, E\right)\ \Sigma_f\left(r, E\right) E_{fission}\, dE\, dr \tag{52}$$

where $v$ is the neutron velocity and $E_{fission}$ is the energy released per fission event. The quantity $S^{'}[t]$ in Equation 50 can be found at each time step by scaling the quantity $S[t]$to the steady-state solution of Equations 50 & 51 for $S^{'}[t]$ at 3,000 MW. With the source term and total reactivity known, Equations 50 and 51 can be solved for the fission power level, $P[t]$ , and the scaled precursor populations, $C_j^{'}[t]$ , for each of the six delay neutron groups.

In the thermal system, once the axial power distribution is known, Equations 34-38 can be solved for the axial temperature distributions of the fuel, gap, cladding and coolant. The location of the maximum temperature in each radial region and its corresponding temperature is calculated to determine if maximum temperature limits have been exceeded. The maximum temperature in the coolant occurs at the outlet of the fission core. Coolant at this temperature is fed into the heat exchanger. Equation 47 governs the amount of heat removed at each time step and allows for the inlet temperature to the core to be calculated.

Finally, once average fuel and coolant temperatures are calculated, reactivity feedbacks for the neutron kinetics system are determined for the next time step. This process is repeated for a predetermined amount of time for equal time steps or until the fuel and

coolant begin to fail, the core is effectively cooled to zero power or the reactor reaches a new steady-state equilibrium. To verify the accuracy of the calculations performed in TAPAS for all three systems, hand calculations of the governing equations were compared with results from the calculational model for various changes in the ion fueling rate, number of source neutrons and fission power level. All transients modeled are examined on the delayed neutron time scale utilizing the prompt jump approximation.

# CHAPTER IV

# RESULTS

In order to fully understand how different transients affect SABR, it is first necessary to look at SABR's typical operating parameters at steady-state. Table 8 illustrates the temperatures throughout the reactor during normal 3,000 MW operation. Figure 8 gives the axial temperature distribution across the fuel pin.

Two criteria are used to determine if the core has reached limiting conditions: coolant boiling and fuel melting, which occur at 1,156 K and 1,473 K, respectively. The melting temperature of the cladding, which is 1,800 K, is not considered as both the coolant and fuel will fail before the cladding melts. For all transients modeled, the time from the beginning of the accident until these failure conditions are met is considered to determine how much time would be available to take correction measures. Two types of accidents are simulated to determine the level of safety that exists in SABR: accidents that affect the neutron population and accidents that disrupt the heat removal system. The accidents that affect the neutron population in the fission core are:

- Increases in plasma auxiliary heating;
- Increases in plasma ion fueling rate, and;
- Reactivity Insertions.

Examples of reactivity insertions include control rod withdrawal. The accidents that affect SABR's heat removal capabilities are:

- Loss of coolant mass flow;
- Loss of heat sink, and;
- Loss of power accidents.

Because the model used cannot predict the effect that exposed fuel will have on the heat removal properties and neutron kinetics of the fuel, loss of coolant accidents leading to the partial or complete uncovering of fuel are not considered in this study. Accidents will be calculated on short time scales on the order of minutes. Due to the lack of detail on the primary loop's piping system such as diameters, heights and friction coefficients, it is impractical to simulate the accidents for longer time periods as natural circulation cannot be taken into account.

Initiating events such as a decrease in coolant velocity will always cause changes in one or more of SABR's three major systems: the fusion neutron source, the fission core and the heat removal systems. Any change, whether small or large, in SABR's main systems will lead to feedbacks that further modify the system dynamics. As discussed in Section 3.2, an increase in fuel temperature will introduce a negative reactivity to the fission core while an increase in coolant temperature will introduce a positive reactivity and increase the fission power. In the fusion core, increases in the ion and electron densities, which are usually very similar, and increases in the plasma ion density will increase the radiative power loss in the plasma. The Troyon Beta Limit and Greenwald Density Limit, which are discussed in Section 3.1, provide an upper limit on the plasma ion density and if exceeded, will force the plasma to shut down.

**Table 8:** Steady-State Operating Conditions

| | Temperature (Kelvin) |
|---|---|
| Coolant Inlet | 650.1 |
| Coolant Outlet | 922.8 |
| Max Cladding | 927.5 at the outlet |
| Max Fuel | 968.8 at 0.63 m above core mid-plane |
| Average Coolant | 786.4 |
| Average Cladding | 796.8 |
| Average Gap | 812.1 |
| Average Fuel | 832.9 |

In order to fully understand how different transients affect SABR, it is first necessary to look at SABR's typical operating parameters at steady-state. Table 8 illustrates the temperatures throughout the reactor during normal 3,000 MW operation. Figure 8 gives

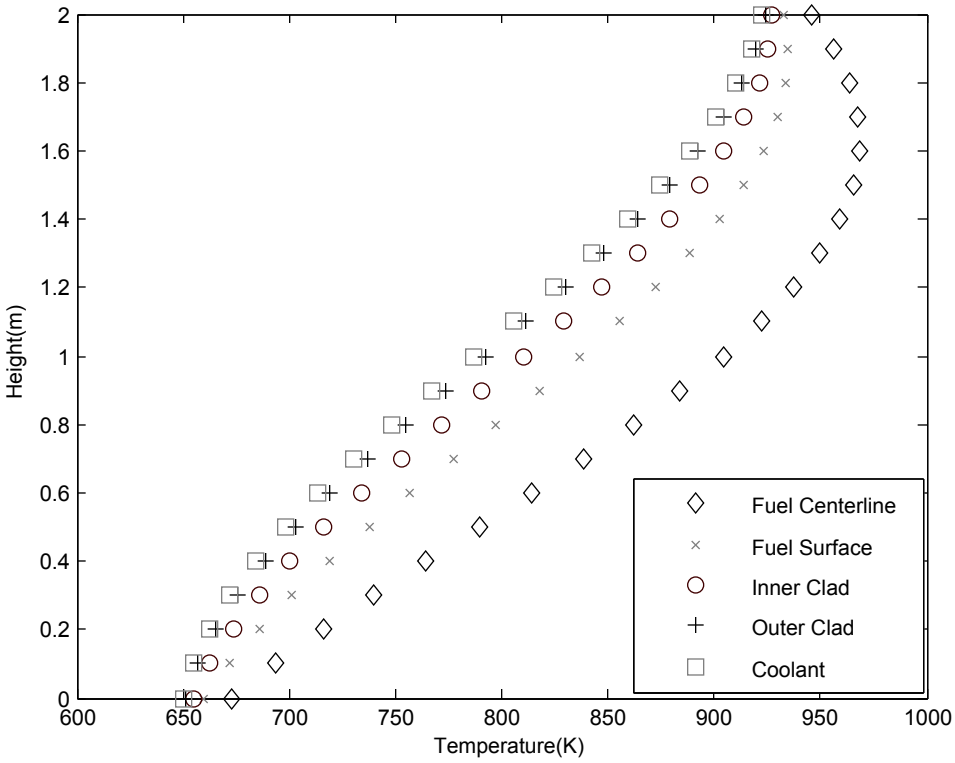


**Figure 8:** Axial Steady-State Temperature Distribution Across SABR Fuel Pin

the axial temperature distribution across the fuel pin.

### *4.1 SABR Control*

In the event that an accident does occur in SABR, the power level in the fission core must be controllable. There are a few methods to controlling the SABR's power level. The first method studied involves control rod insertion. A control rod worth of -9$, which is the total reactivity worth of SABR's sixteen control rods, would be sufficient to shut down a critical reactor but in a source-driven subcritical reactor control rods will only lead to a lower steady-state power level. Poison injection into the fission core was not included in the design of SABR but would lead to the same results as control rod insertion. For $k_{eff}$ = 0.95, a full control rod insertion worth -9$ of reactivity reduces the power level by 33%. To illustrate that more control rods are not sufficient to shut down the reactor, it would take another 36$ of reactivity to bring the reactor down another 33% of the original power. At lower levels of multiplication, such as $k_{eff} = 0.829$ during EOC, nine dollars of negative

reactivity leads to a power reduction of only 11%. The closer the reactor is to critical, the more effective control rods are but with the neutron source running, it will be impossible to bring the power to zero. Because control rods are not an effective method to shutting down the reactor, they are only valuable for fine control of the fission power level.

The preferred option for shutting down the reactor is turning off the neutron source. There are three options to do this:

- Impurity injection;
- Decreasing the plasma ion fueling rate, and;
- Turning off the plasma auxiliary heating.

Impurity and plasma ion injections are represented as occurring linearly over five seconds as a conservative approximation of the complex physical processes involved. Changes in the plasma auxiliary heating rate are simulated as instantaneous increases or decreases.

Injecting impurities into the plasma will causes the radiation power loss term in Equation 10 to increase and thus the fusion power level to decrease. Figure 9 illustrates the fusion power response due to Carbon and Tungsten impurities injection into the plasma over 5 seconds. While the fusion power does decay fairly quickly and would be useful in controlling the plasma, it does take a few tens of seconds to equilibrate and is thus not the best method to shut down the neutron source.

The next method for shutting down the fusion neutron source is through control of the plasma ion fueling rate. Figure 10 illustrates the fusion power response to the plasma ion fueling rate decreasing over 5 seconds. Decreasing the plasma ion density is a very effective method for modulating the fusion power and would be a good backup system for shutting down the neutron source. The only disadvantage for this option is that escaping plasma particles will recycle from the first wall back into the plasma, which occurs over a longer period of time than it takes to turn off the plasma by shutting down the auxiliary heating. The case of an accidental increase in plasma fueling will be examined later.

The preferred method to shut down the plasma and thus turn off the reactor is to turn off the auxiliary heating to the plasma. Figures 11 & 12 illustrate the fusion and fission

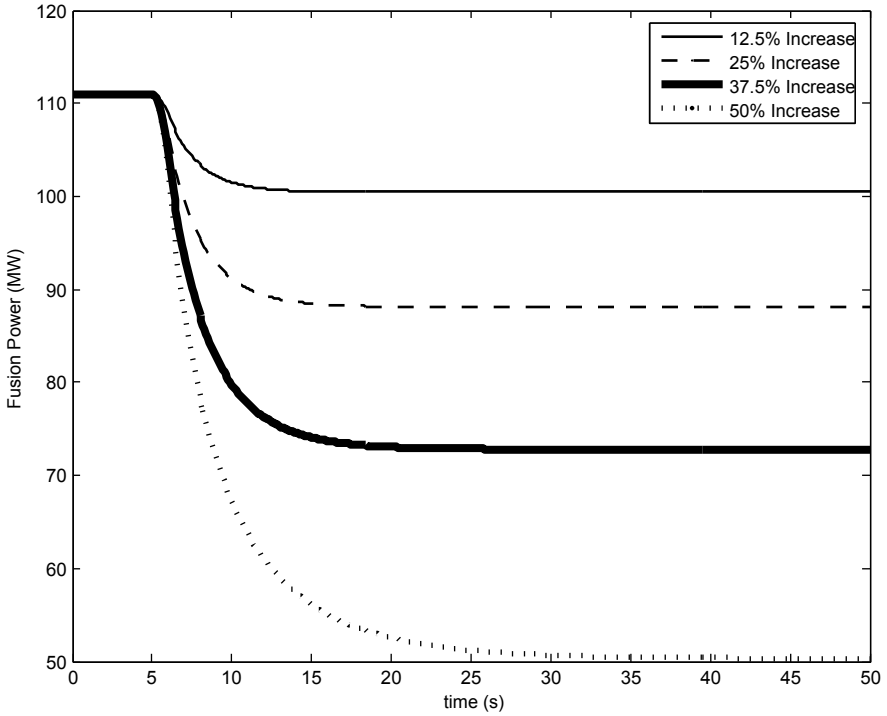


**Figure 9:** Fusion Power Level during Carbon and Tungsten Impurity Injection at BOL

power levels after plasma auxiliary heating shutdown. The power levels decay on the energy confinement time scale of about one second. Once the external heating drives are turned off, the plasma power will decay to zero in approximately three seconds. Without the aid of source neutrons in the subcritical fission core, the prompt neutrons will die away proportionally to the neutron source leaving only a fraction of the original power due to decay heat and delayed neutrons. The delayed neutrons have a half life of less than a minute but ten minutes after the plasma auxiliary heating is turned off there will be still be 3% power in the form of decay heat. A day later, the decay heat will be less than 1%. Decay Heat effects without the heat removal systems are discussed in depth later for Loss of Heat Sink and Loss of Power Accidents. Fine control of the fusion neutron source can be achieved through modulation of the fuel or impurity ion densities but the plasma auxiliary heating is the best method to shut down the neutron source due to the plasma's rapid response to any change in the auxiliary heating.

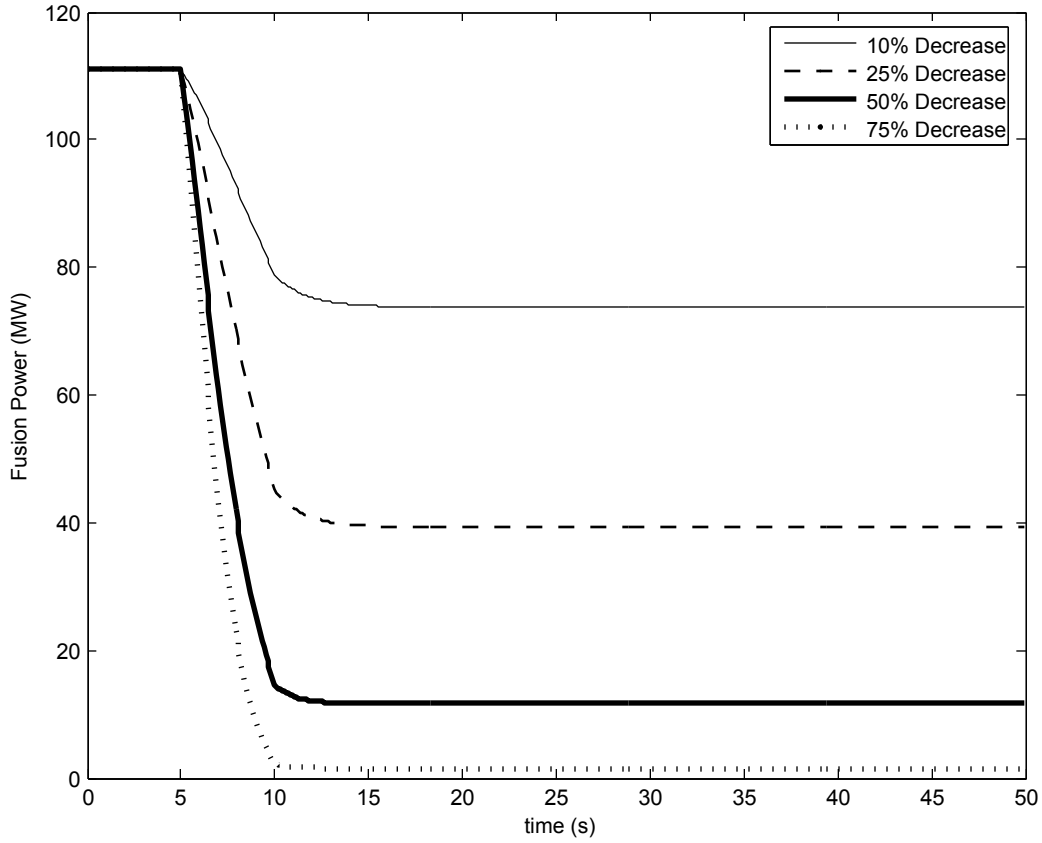


**Figure 10:** Fusion Power Level during Ion Fueling Rate Decrease at BOL

## *4.2 SABR Transients Affecting the Neutron Population*

### 4.2.1 Accident Scenario One: Increase in Plasma Auxiliary Heating

With only a couple of the six 20 MW auxiliary heating drives for SABR's fusion core on at any given time, it is possible that one of them could accidentally turn on. While it is highly improbable that an extra heating drive could spontaneously turn on, the result leads to a rapid increase in the fusion power level and thus requires attention.

The worst case scenario for one auxiliary heating drive accidentally turning on is during BOL operation when one extra heating drive would change the auxiliary heating to the plasma from 40 to 60 MW. With $k_{eff} = 0.95$ at BOL, the fusion power increases from 111 MW to 157 MW, which increases the fission power to 4,288 MW from 3,000 MW. In the absence of any control action, the maximum fuel temperature increases to 1,142 K and the maximum coolant temperature increases to 1,079 K, which are both below their respective

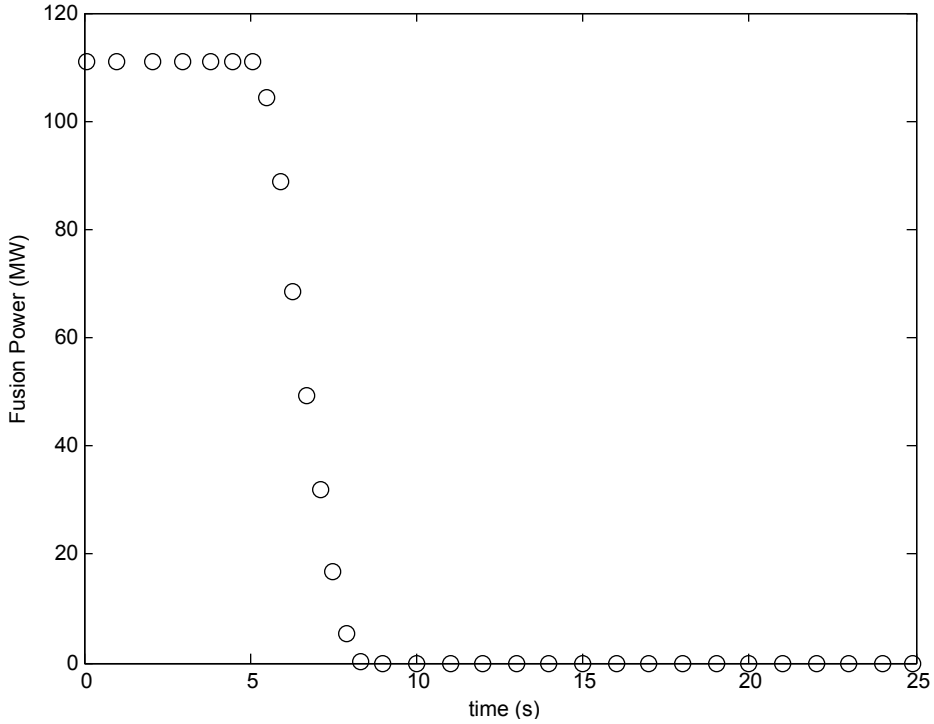


**Figure 11:** Fusion Power Level during Removal of Auxiliary Heating to Plasma at BOL

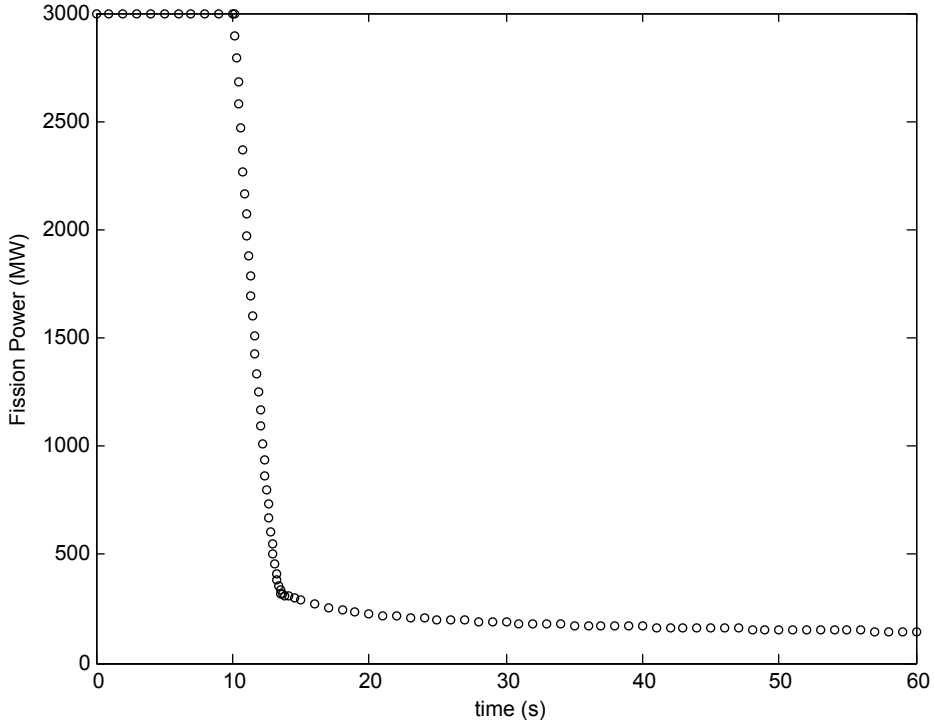


**Figure 12:** Fission Power Level during Removal of Auxiliary Heating to Plasma at BOL

failure temperatures of 1,473 and 1,165 K. Because of the rapid response of the fusion power to changes in the auxiliary heating, power levels and temperature profiles rise quickly on the order of seconds. For 20 MW of additional auxiliary heating at BOL operation, neither the Troyon Beta nor the Greenwald Density Limits are surpassed.

For an additional 20 MW plasma auxiliary heating during both BOC and EOC operation, however, the Troyon Beta Limit is surpassed and plasma confinement is lost, which shuts down the fusion neutron source and thus the fission core. Due to the Troyon Beta Limit during BOC and EOC operation, SABR is able to withstand an accidental increase in plasma auxiliary heating without sustaining any permanent damage to the reactor. SABR is consequently capable of withstanding an additional plasma auxliary heating unit turning on without sustaining damage to the reactor. Figure 13 illustrates the maximum temperatures of the fuel, cladding and coolant as well as the coolant inlet temperature to the core during a 20 MW increase in auxiliary heating at BOL. Results for BOC and EOC operation are included in Table 4.2.1 but are not relevant as in all cases they exceed the Troyon Beta Limit.

**Table 9:** Summary of Accidental Plasma Auxiliary Heating Increases

| | BOL | BOC | EOC |
|---|---|---|---|
| Max $T_{coolant}$ for 20 MW Increase in $P_{aux}(K)$ | 1,079 | 968 [a] | 952 [a] |
| Max $T_{fuel}$ for 20 MW Increase in $P_{aux}$ (K) | 1,142 | 1,020 [a] | 1,002 [a] |
| New $P_{fusion}/P_{fission}$ for 20 MW Increase in $P_{aux}$ (K) | 157/4,288 | 207/3,382 [a] | 237/3,248 [a] |
| Max $T_{coolant}$ for 40 MW Increase in $P_{aux}(K)$ | 1,184 [a] | 1,003 [a] | 976 [a] |
| Max $T_{fuel}$ for 40 MW Increase in $P_{aux}$ (K) | 1,259 [a] | 1,058 [a] | 1,028 [a] |
| New $P_{fusion}/P_{fission}$ for 40 MW Increase in $P_{aux}$ (K) | 185/5,132 [a] | 225/3,666 [a] | 253/3,445 [a] |

[a] Troyon Beta Limit is exceeded

### 4.2.2 Accident Scenario Two: Increase in Plasma Ion Density

An accidental increase in the plasma fueling rate would lead to a new equilibrium ion density and a higher fusion power. With more source neutrons streaming into the fission core, the

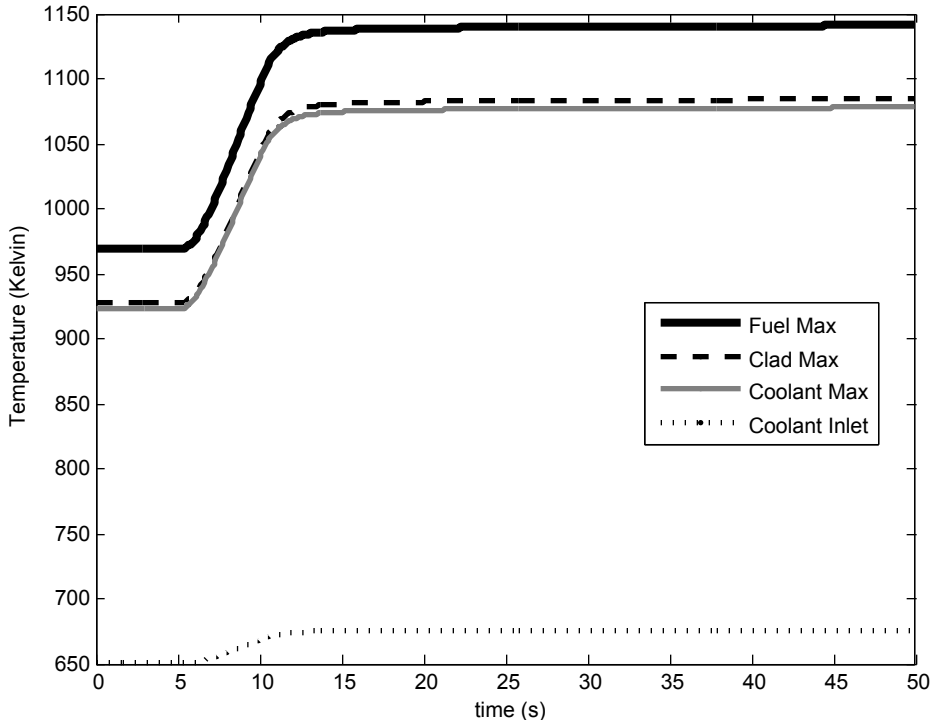


**Figure 13:** Maximum Temperatures During Increase in Auxiliary Heating from 40 to 60 MW at BOL

fission power will increase leading to higher temperatures in the core. For the calculations that follow, the fueling rate increases linearly over five seconds.

Figures 14 & 15 illustrate the effect that different increases in the plasma ion density have on the fusion power and fission power levels. Figure 16 illustrates this effect on the temperatures in the core. At BOL, SABR can sustain up to an 11% increase in the plasma ion density, which corresponds to an 18% increase in the plasma ion fueling rate. For an ion density increase of 12% of more, there would be at most 46 seconds after the beginning of the transient to take corrective measures before the coolant exceeds its boiling temperature of 1,156 K. SABR's fuel will begin to melt at an ion density increase of greater than 19%, or a 28% increase in the plasma ion fueling rate, with no more than 14 seconds to take corrective measures from the start of the accident. Fortunately, during BOL operation, the Troyon Beta Limit is exceeded for a plasma ion density increase of 11%. This prevents any accidental ion density increases from causing damage to SABR.

For BOC fuel composition with $k_{eff} = 0.879$ and the required fusion power of 183 MW,

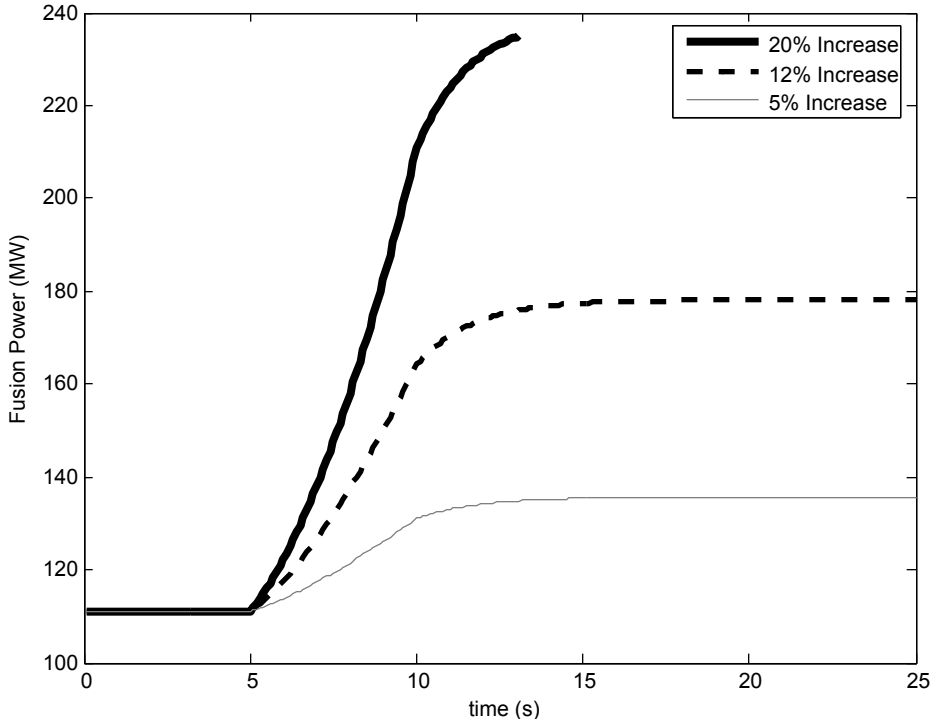


**Figure 14:** Fusion Power Level with Increase in Plasma Ion Density at BOL

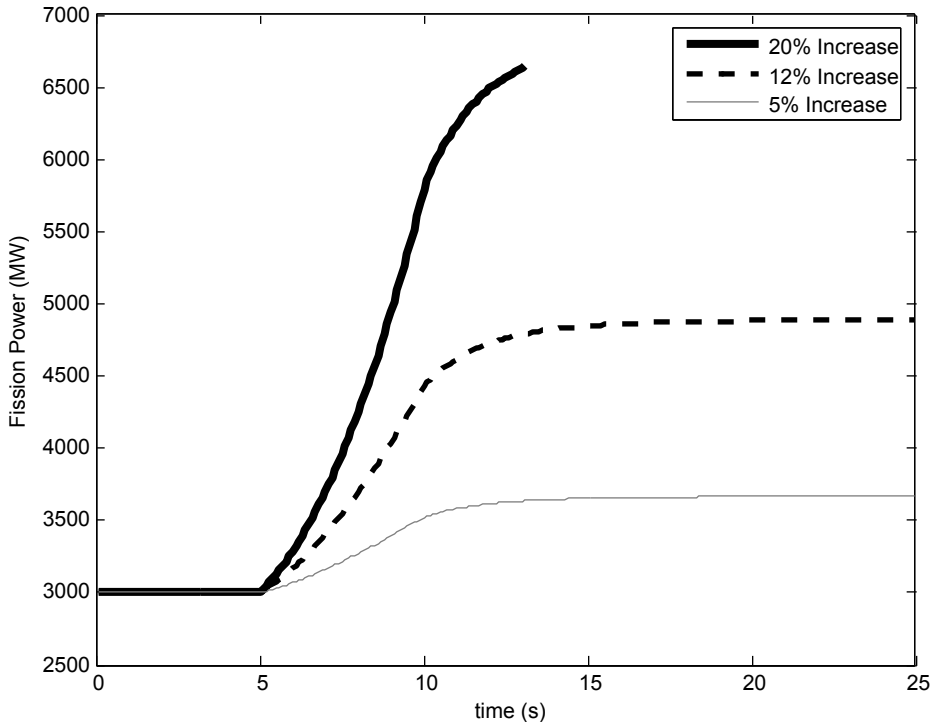


**Figure 15:** Fission Power Level with Increase in Plasma Ion Density at BOL

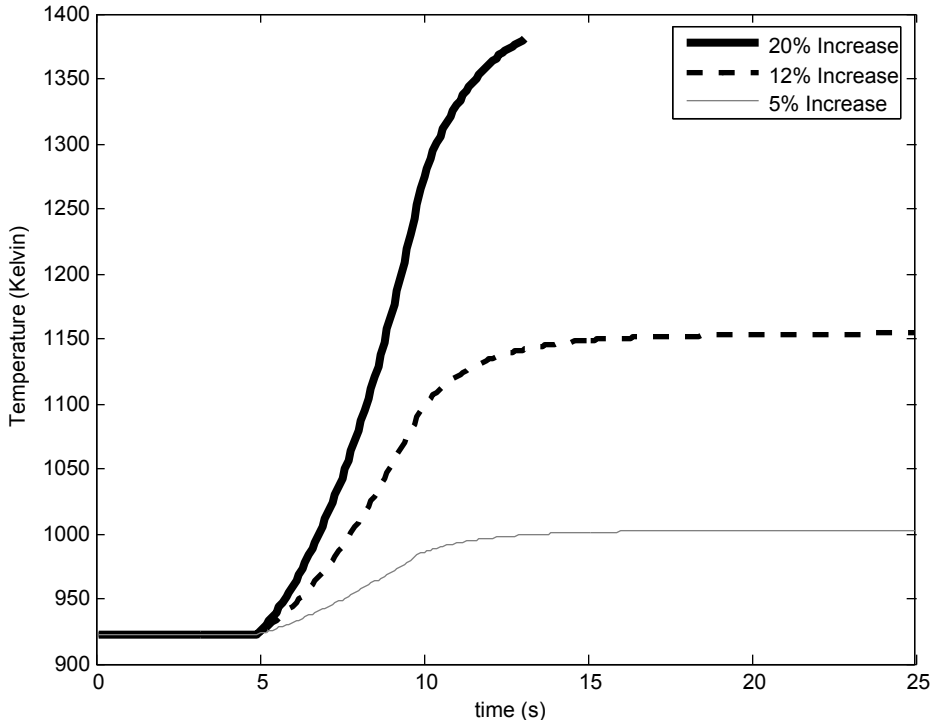


**Figure 16:** Maximum Coolant Temperature with Increase in Plasma Ion Density at BOL

SABR can sustain up to a 17% increase in plasma ion density, corresponding to a 22% increase in the plasma ion fueling rate, before coolant boiling occurs when unconstrained by plasma density limits. During EOC fuel composition with $k_{eff} = 0.829$ and the required fusion power of 218 MW, SABR can sustain up to a 19% increase in plasma ion density, corresponding to a 22% increase in the plasma ion fueling rate, before coolant boiling occurs without density limits taken into account. Fuel melting occurs for BOC and EOC operation at a 29% and 32% increase in plasma ion density, respectively. Times until fuel melting and coolant boiling for BOC and EOC operation are comparable to the times for BOL operation. Due to operation near the Troyon Beta Limit, during both BOC and EOC operation, the Troyon Beta Limit is exceeded before either the coolant or fuel begins to fail and SABR shuts down without any reactor damage. As seen in Table 10 below, all accidental increases in plasma ion density that would lead to fuel or coolant failure are preceded by the Troyon Beta Limit being surpassed. However, despite the safety offered by the density limit, more attention needs to given to the plasma fueling system design to prevent inadvertent fueling increases. This is especially true for BOL operation when the margin between damage to

SABR and the Troyon Beta Limit being exceeded is very small. It is also important to note the importance of operating SABR's neutron source close to the Troyon Beta Limit to prevent damage to the reactor from accidental plasma ion density increases.

**Table 10:** Summary of Accidental Plasma Ion Density Increases

| | BOL | BOC | EOC |
|---|---|---|---|
| Maximum Plasma Ion Density Increase Before Coolant Failure | 12% | 17% | 19% |
| Corresponding Plasma Ion Fueling Rate Increase | 18% | 22% | 22% |
| Time Until Coolant Failure (seconds) | 46 | 29 | 27 |
| Maximum Plasma Ion Density Increase Before Fuel Failure | 19% | 29% | 32% |
| Time Until Fuel Failure (seconds) | 14 | 13 | 16 |
| Maximum Plasma Ion Density Increase Before Troyon Beta Limit is Exceeded | 11% | 1% | 2% |

### 4.2.3 Accident Scenario Three: Reactivity Insertion

Unlike critical reactors, a small reactivity insertion in SABR, due to control rod removal for example, does not lead to supercriticality and a runaway chain reaction. Instead, the reactor will equilibrate to a higher power level as long as criticality is not achieved. During steady-state BOL operation, SABR's reactivity is -17.5\$. If the 16 control rods were fully inserted, SABR's reactivity drops to -26.5\$ with $k_{eff} = 0.926$. To maintain 3,000 MW, the fusion neutron source would need to be increased from 111 to 167 MW. Were the control rods to be fully removed at this point and $k_{eff} = 0.95$ reestablished, the new steady-state power level would be 4,609 MW, as illustrated in Figure 17, with an outlet coolant temperature of 1,119 K, which is just below the sodium boiling point. Therefore, SABR is capable of withstanding this event without sustaining damage to the reactor.

At BOL, an instantaneous reactivity insertion equivalent to the ejection of one control rod corresponds to 0.56\$ and a power increase of 99 MW while the coolant outlet temperature rises 12 K. Other scenarios for reactivity insertions were not considered as credible situations of added fuel or neutron reflection in the fission core that do not disrupt the fusion neutron source could not be contemplated.

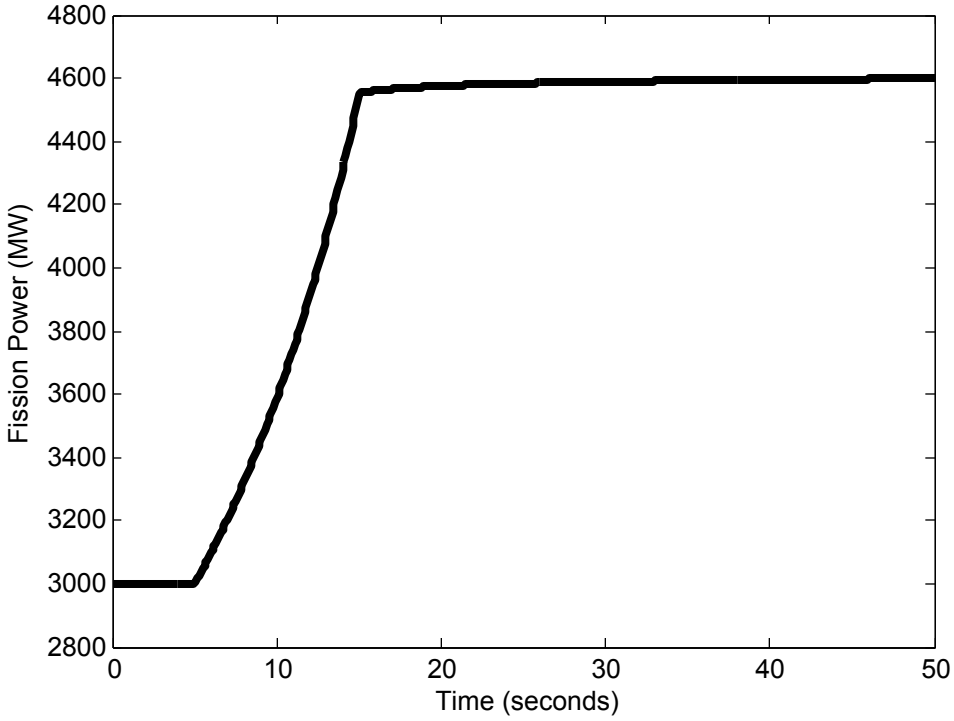


**Figure 17:** Ten Second Removal of All Control Rods at $k_{eff} = 0.926$

## *4.3 SABR Transients Affecting Heat Removal Capability*

### 4.3.1 Accident Scenario One: Loss of Coolant Mass Flow

A Loss of Flow Accident (LOFA), often due to coolant pump failure, is a particularly dangerous accident for any reactor. With coolant mass flow across the fuel either decreased or halted entirely and the neutron source remaining on, the heat produced in the fuel rods is not being removed effectively from the reactor core and temperatures will begin to increase. For a reactor with a large negative reactivity feedback, the fission power level will decrease significantly. Unfortunately, the Doppler Coefficient in SABR, while negative, is small and overwhelmed by the positive sodium voiding coefficient, which will lead to an increase in the fission power level. If the reactor's fuel and coolant do not fail, eventually the reactor will reach an equilibrium state where the power being produced in the core, which is larger due to reactivity feedbacks, is removed in the heat exchanger. For all loss of flow accidents examined, the coolant began to boil before the fuel began to melt. Table 11 lists the times until failure for both the coolant and fuel for various LOFA. Failure times for the

fuel conserve the coolant temperature increases but ignore the coolant's phase change from liquid to gas.

The rate at which the coolant mass flow rate decays is a function of the energy loss due to the pump work and the kinetic energy of the pump. Without an accurate design of SABR's pumps, a halving time of twenty-five seconds was chosen for the coolant mass flow rate decay, shown below in Equation 53, where $LOFA_{fr}$ is the fraction of the original value that the coolant mass flow rate decays to and $t$ is the time since the start of the accident. Flow halving times of up to fifty seconds have been suggested for Superphénix [6] and similar liquid metal fast breeder reactors [14] but half this value was chosen as it is a conservative estimate. All loss of flow accidents are described in terms of the percentage of the original coolant mass flow rate that is lost such that a 10% LOFA represents coolant flow at 90% of the original mass flow rate.

$$v\left(t\right) = v_0 \left( LOFA_{fr} + \left(1 - LOFA_{fr}\right) e^{-\frac{ln(2)}{25}t} \right) \tag{53}$$

For BOL fuel where $k_{eff} = 0.95$, SABR can sustain a 48% LOFA before the coolant begins to boil. During a 49% LOFA, the coolant will boil 156 seconds after the start of the transient. For larger decreases in the coolant flow rate, the coolant will fail earlier. For an 80% LOFA, coolant will boil after 34 seconds while during a complete loss of flow accident, the coolant boils after 24 seconds. Figure 18 illustrates the temperature response within the fuel pin to a change in the coolant mass flow rate. Figures 19 & 20 show the maximum fuel and coolant temperatures during different LOFAs and Figure 21 illustrates the fission power's response to the these temperature changes in the form of reactivity feedbacks. The temperature and power curves for larger flow losses are cut off when both the fuel and coolant have failed. It is important to note that Figure 18 illustrates a decrease in the coolant inlet temperature during a loss of flow accident. This is not a true representation of what would happen during this situation but is an artifact of the TAPAS code due to the lack of detailed modeling of the heat exchangers.

For BOC fuel composition, the coolant will boil during a 50% loss of flow 161 seconds after the start of the accident if no control action is taken. During EOC operation, the

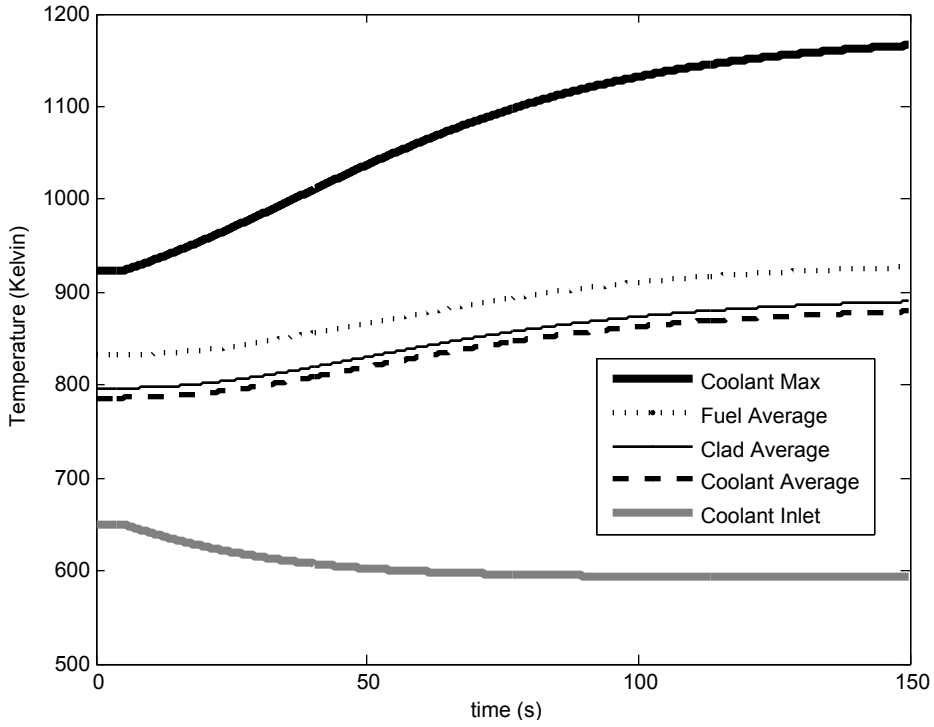


**Figure 18:** Average Fuel Pin Temperature Distribution during 50% Loss of Flow Accident at BOL

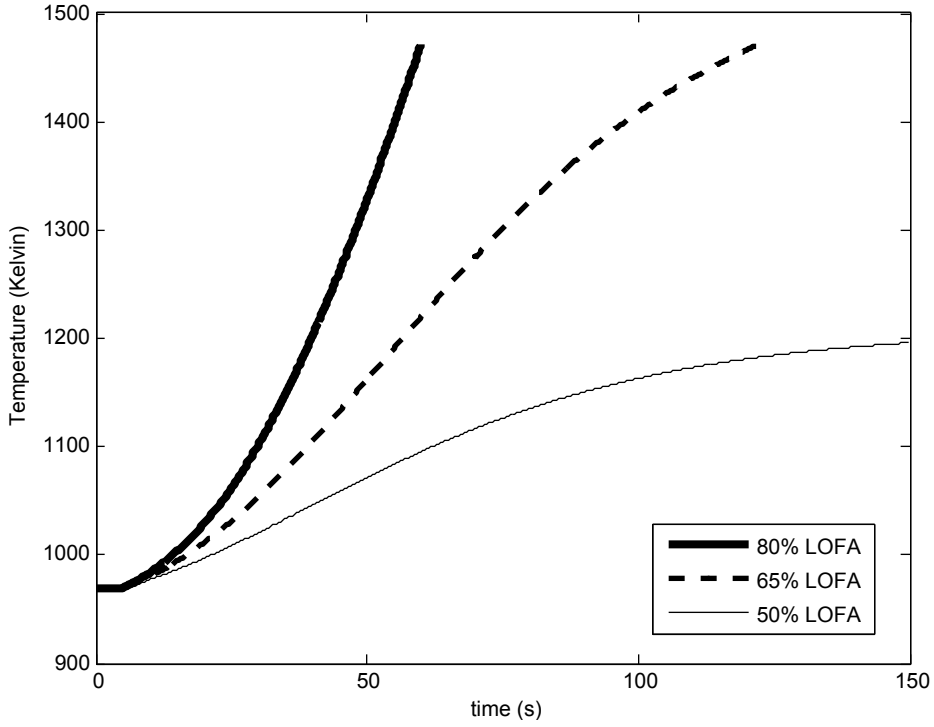


**Figure 19:** Maximum Fuel Temperature during Loss of Flow Accident at BOL

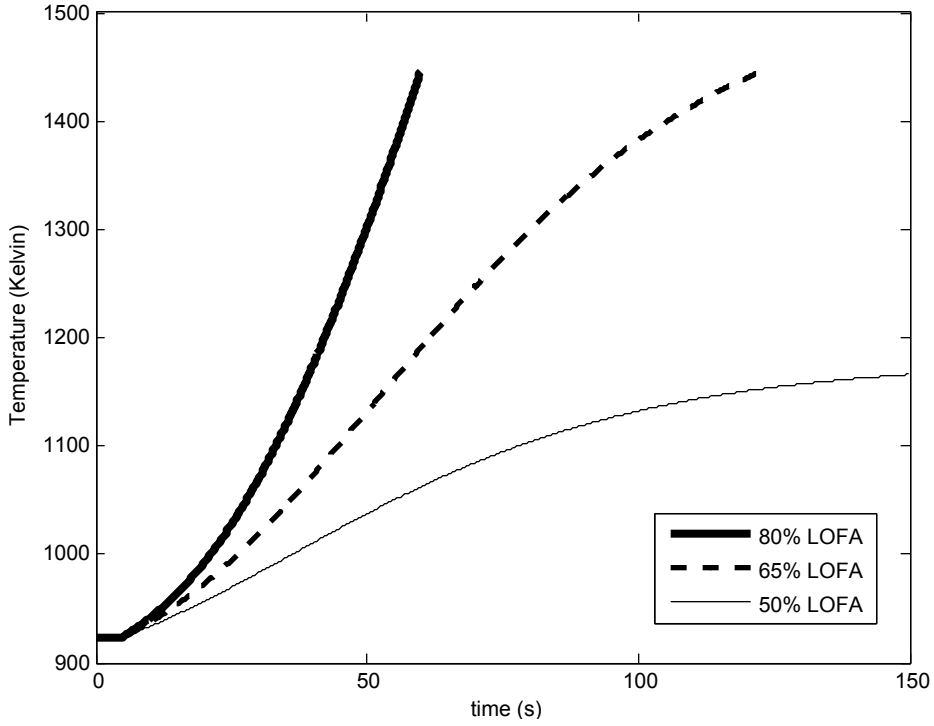


**Figure 20:** Maximum Coolant Temperature during Loss of Flow Accident at BOL

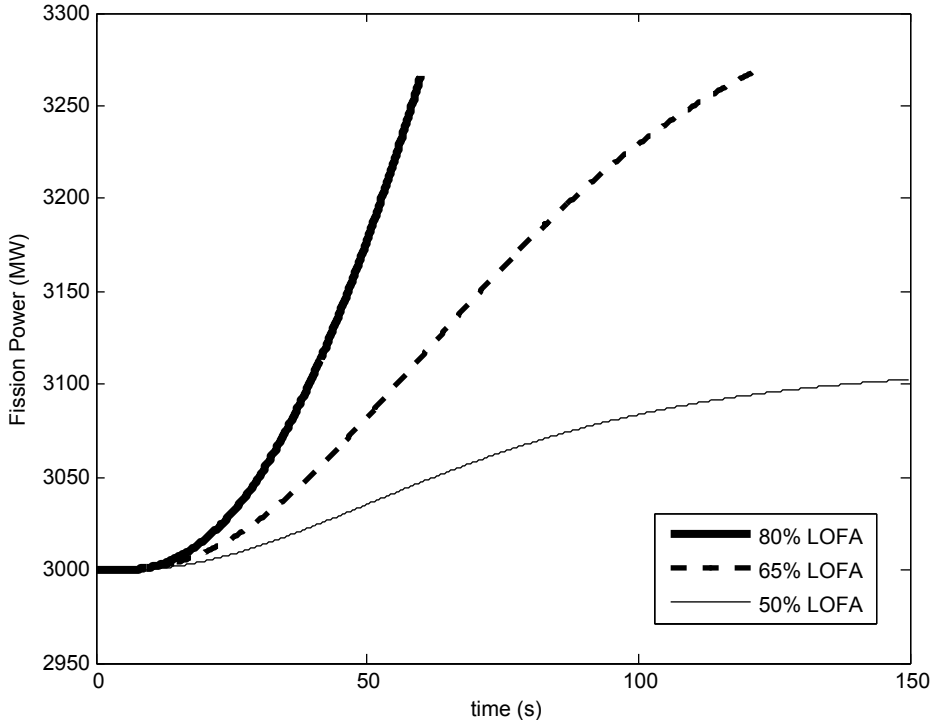


**Figure 21:** Fission Power during Loss of Flow Accident at BOL

coolant will fail at the same flow rates as for BOC operation but after 178 seconds instead. These times to failure are sufficiently long so as to provide adequate time for detection of the accident and for control action to be taken to shut down the neutron source. For very large and complete loss of flow accidents, BOC and EOC results are similar to BOL results. During an 80% LOFA, the coolant will boil after 35 seconds for both BOC and EOC fuel composition. A complete loss of flow for both BOC and EOC fuel compositions leads to coolant failure after 25 seconds. It is important to note that a complete loss of flow accident is unlikely due to the presence of natural circulation. However, without accurate modeling of the piping system, this cannot be simulated. Pump failure in SABR, if left unchecked, can quickly cause irreparable damage to the reactor. The best method of dealing with a Loss of Flow Accident is shutting down the plasma, which is best accomplished by turning off the plasma auxiliary heating. Once the neutron source is turned off, the power level in the fission core will very quickly decrease to decay heat levels. The dynamics of SABR during the decay heat removal (DHR) phase for decrease coolant mass flow rates are examined later in the Loss of Power section.

During less severe loss of flow accidents, the time to take corrective measures increases to a few minutes, which is more than enough time for operators to react. For all fuel compositions, SABR is able to sustain small coolant mass flow rate changes and will only be at risk of serious damage for pump failures of approximately 50% or more. If pumping power is significantly decreased, auxiliary generators should be used to restart the pumps and provide coolant flow to remove decay heat production. Similar to the treatment for an accidental increase in plasma auxiliary heating, using a large number of small pumps in the primary coolant loop will decrease the probability of large loss of flow accidents, especially if the pumps are operating on separate systems. In the Superphénix reactor, four independent loops with their own pumps were utilized so that if one loop failed, the other three could maintain a safe coolant flow rate [6]. And in the unlikely event that all four pumping systems failed, auxiliary motors continue to pump the coolant, although at a reduced rate, through the core.

Engineering the pipes leading from the coolant pumps into the reactor core is a difficult

task when designing a reactor that is more complicated in SABR due to the annular core and central solenoid region. The problem is getting the coolant to mix in the structural diagrid under the fuel rods so that if one coolant loop flow all fuel rods have sufficient coolant flow to remove the heat being produced. Future work performed on designing SABR's heat removal system must ensure that a loss of pumping power in a coolant loop does not lead to stagnant coolant in any reactor region.

**Table 11:** Loss of Flow Accident Summary

| | BOL | BOC | EOC |
|---|---|---|---|
| LOFA where Coolant Boiling first occurs | 49% | 50% | 50% |
| Time Until Coolant Boiling (seconds) | 156 | 161 | 178 |
| LOFA where Fuel Melting first occurs | 63% | 65% | 65% |
| Time Until Fuel Melting (seconds) | 177 | 183 | 151 |
| Time Until Coolant Failure for Complete LOFA (seconds) | 24 | 25 | 25 |
| Time Until Fuel Failure for Complete LOFA (seconds) | 36 | 38 | 38 |
| Maximum LOFA Tolerable for Complete Decay Heat Removal | 93% | 93% | 93% |

### 4.3.2 Accident Scenario Two: Loss of Heat Sink

An uncontrolled Loss of Heat Sink Accident, or LOHSA, is the result of a failure in the intermediate or secondary loops leading to a decrease in the overall heat transfer coefficient of the heat exchanger. This decrease could be caused by a break in the intermediate loop, a loss of flow in the intermediate loop or a steam generator failure. With less heat removal, the temperature of the coolant leaving the heat exchanger in the primary loop will increase, which therefore increases the temperature of the coolant at the inlet to the core and across the fuel pin. As with the Loss of Flow Accident, an increase in coolant temperature leads to a positive sodium voiding reactivity feedback and thus further increases in core temperatures as the fission power level rises. Table 4.3.2 lists the results of various loss of heat sink accidents, including the time until fuel melting, which occurs after the onset of coolant boiling in all LOHSA. Times until fuel melting conserve the coolant temperature increases but ignore the coolant's phase change from liquid to gas. Unless otherwise stated, the neutron source remains on during these accident scenarios.

Because SABR's heat removal system was not designed in sufficient detail to allow detailed analysis beyond the heat exchanger, a model similar to the Loss of Flow Accident was used where the overall heat transfer coefficient of the heat exchanger decays over time to a lower value. To simulate this accident, a halving time of ten seconds was chosen for the decay period of the heat exchanger heat transfer coefficient. All loss of heat sink accidents are described in terms of the percent decrease in the overall heat transfer coefficient of the heat exchanger.

For BOL operation, the coolant will first start boiling during a 33% LOHSA 65 seconds after the start of this transient. For more severe LOHSA, the coolant will fail much faster. During a 70% LOHSA, the coolant will boil after 10 seconds. Figure 22 illustrates the response of the temperature distribution across the fuel pin for a 25% LOHSA. Figures 23-25 illustrate the maximum fuel and coolant temperatures and fission power responses during various LOHSA.

During BOC operation, coolant boiling initially occurs for a 36% LOHSA 70 seconds after the start of the accident. For EOC operation, coolant failure also occurs for a 36% LOHSA but after 78 seconds instead. For a 70% LOHSA, coolant boiling for BOC operation occurs after 11 seconds. There are 11 seconds until coolant failure during EOC operation for a 70% LOHSA.

There are approximately 10 seconds to take corrective measures for a worst case scenario LOHSA, or complete loss of heat sink. However, this worst case scenario is hypothetical and unrealistically pessimistic; the intermediate loop's coolant pipes would need to be voided nearly instantaneously, most likely caused by a large pipe break. Also convective heat transfer from the coolant pipes to the atmosphere will always be present. As with existing sodium cooled reactors, independent coolant loops working in parallel should be utilized so that in case one breaks, the remaining loops can remove the necessary heat while corrective measures are taken. For example, Superphénix's four independent loops each have two heat exchangers per coolant loop [6]. In the event that all of the heat exchangers fail, sodium-to-air coolant loops should be used to remove the heat generated by decay heat. For smaller pipe breaks resulting in less severe loss of heat sink accidents, there are tens of seconds,

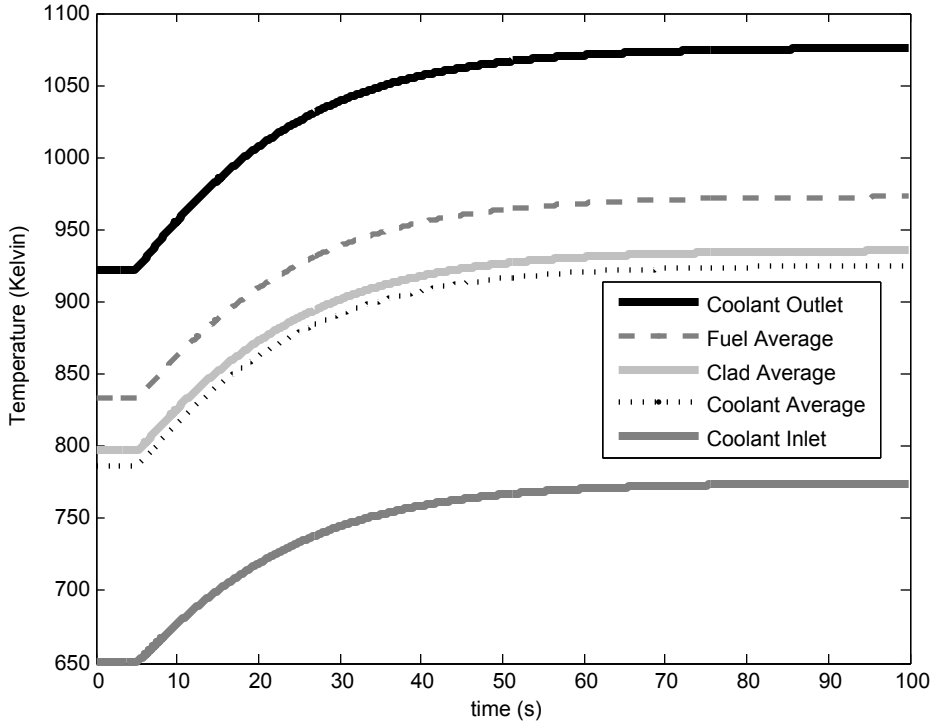


**Figure 22:** Average Fuel Pin Temperature Distribution during 25% Loss of Heat Sink at BOL

sometimes even up to a minute, before corrective measures need to be taken to prevent permanent damage to the reactor. SABR can sustain up to a 33% loss in heat sink without control action before damage will occur. With coolant temperature and pressure monitoring systems that would decrease or shut down fusion power when an accident is detected, this is not a large problem to overcome. Once decay heat is the only power being produced in SABR's core, a LOHSA of up to 70% can be tolerated before the coolant begins to melt. Therefore, the remaining functional heat exchangers and sodium-to-air coolant loops must be capable of providing an overall heat transfer coefficient of 30% of the original value to remove the decay heat.

### 4.3.3 Accident Scenario Three: Loss of Power

A Loss of Power Accident, or LOPA, is an accident where power to SABR's auxiliary systems, namely the coolant pumps and plasma auxiliary heating, is lost. This accident

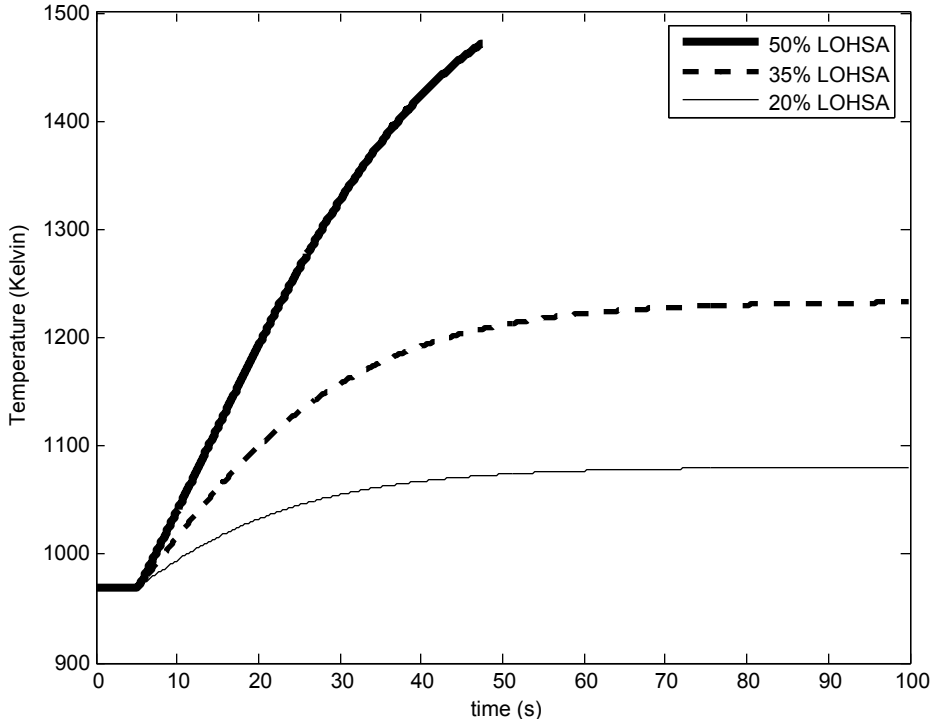


**Figure 23:** Maximum Fuel Temperature during Loss of Heat Sink Accident at BOL

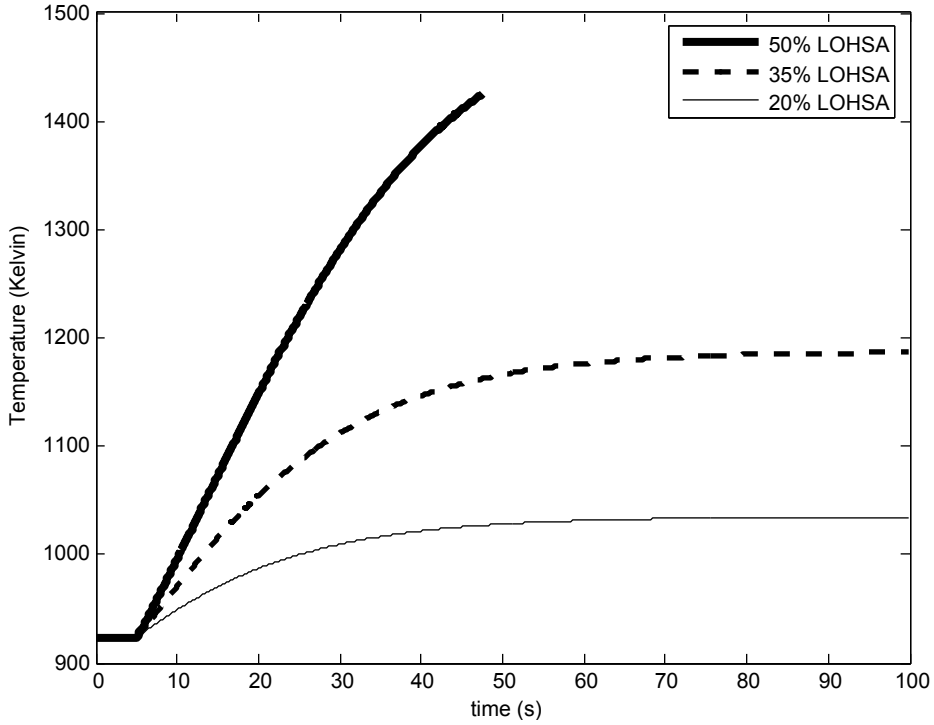


**Figure 24:** Maximum Coolant Temperature during Loss of Heat Sink Accident at BOL

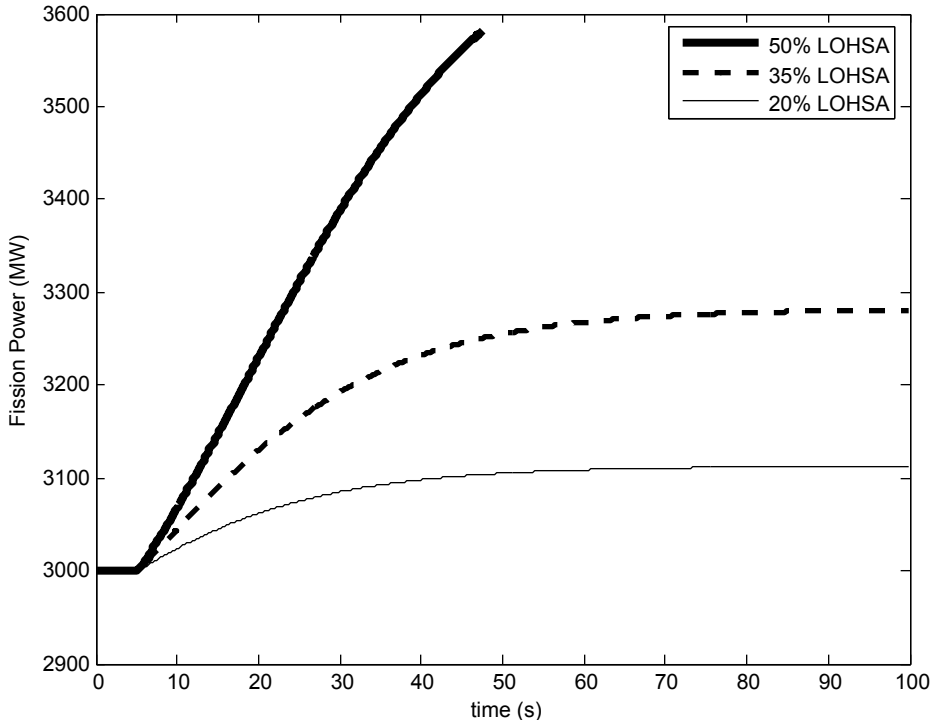


**Figure 25:** Fission Power during Loss of Heat Sink Accident at BOL

is similar to a complete Loss of Flow Accident in which corrective measures are taken immediately. Without functional pumps, the coolant mass flow rate will begin to decay to zero and temperatures in the core will increase. However, when the power to the external plasma heating drives is cut off, the fusion neutron source will shut down almost instantly, as shown in Figure 11. Less than three seconds later the number of source neutrons streaming into the fission core will be zero and the subcriticality of the fission core will cause the neutron population to go to zero as well.

Unfortunately, a neutron population of zero does not mean that the power production in the core is zero. As the fission products decay, a fraction of the original 3,000 MW is produced. Decay heat production in the core is initially 11% and after one hour is 3%. Were the coolant still flowing past the fuel pins, the power generated in SABR would be easily removed. But with the pumps inactive, the coolant's mass flow rate decays to zero meaning that the temperatures continue to build up in the core. As with the Loss of Flow Accident, a halving time of 25 seconds for the coolant mass flow rate was used. Figure 26 below illustrates the response of the average temperatures in the core for the power profile

**Table 12:** Loss of Heat Sink Accident Summary

| | BOL | BOC | EOC |
|---|---|---|---|
| LOHSA where Coolant Boiling first occurs | 33%[a] | 36% | 36% |
| Time Until Coolant Boiling (seconds) | 65 | 70 | 78 |
| LOHSA where Fuel Melting first occurs | 47% | 53% | 54% |
| Time Until Fuel Melting (seconds) | 77 | 87 | 86 |
| Time Until Coolant Failure for 70% LOHSA (seconds) | 10 | 11 | 11 |
| Time Until Fuel Failure for 70% LOHSA (seconds) | 17 | 21 | 22 |
| Maximum LOHSA Tolerable for Complete Decay Heat Removal | 70% | 70% | 70% |

[a]All values are given as percent decrease in overall heat transfer coefficient of the heat exchanger

shown in Figure 12 after auxiliary heating to the plasma is turned off.

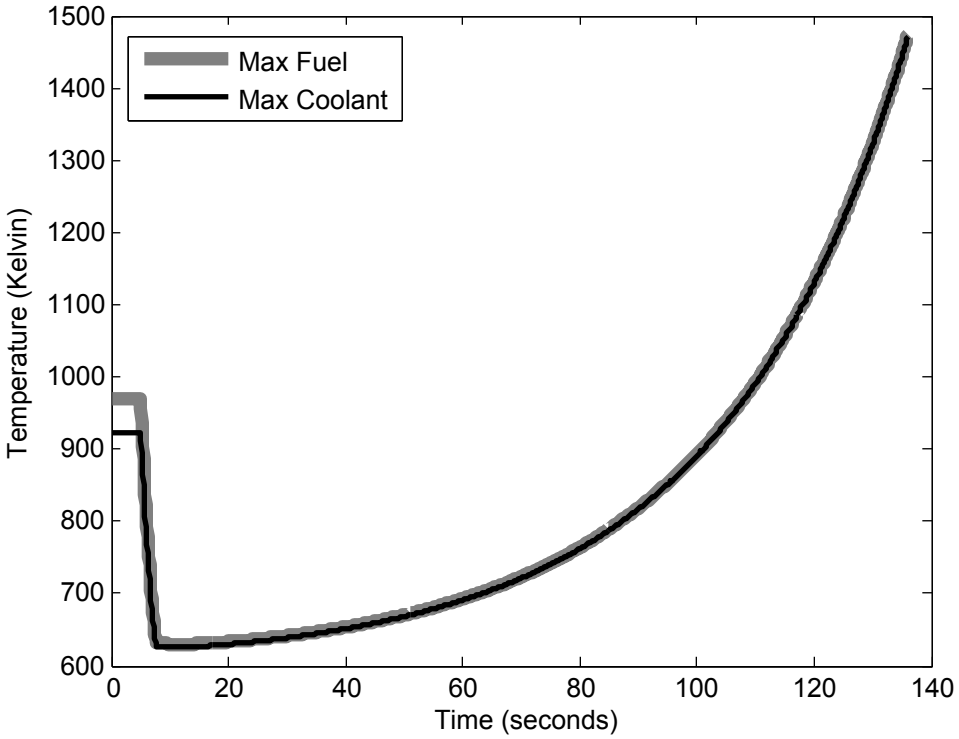


**Figure 26:** Maximum Temperatures in SABR's Core during a Loss of Power Accident at BOL

Once the fission power is approximately zero, reactivity feedbacks no longer lead to extra power production but the small fraction of decay heat power will eventually lead to coolant boiling and fuel melting in the reactor. After two minutes, the temperatures in SABR's

fission core will have increased too much and the reactor will fail. Time until reactor failure is the same for BOL, BOC and EOC operation.

With the pumps shut down and the coolant mass flow rate decaying to zero, an effective way to deal with the decay heat transferring into the coolant must be found. If the core were flooded with colder liquid sodium, decay heat could be removed to prevent fuel melting or coolant boiling. However, there are two problems with this solution. First, the sodium reserve must be kept in liquid form for the entire lifetime of the reactor, which would require an unnecessary waste of energy. Second, the core would have to be reflooded with new sodium every two minutes over the course of a few days and it is impractical to keep a reserve sodium inventory this large.

In conventional nuclear reactors, large diesel or battery powered generators are used to restart the pumps in the event of pump failure or a loss of power accident. If the pumps to the primary and intermediate loops are restarted, the decay heat can be effectively removed. These generators will be expensive and require large amounts of energy but they will effectively prevent a loss of power accident from causing permanent damage to SABR. During the decay heat removal phase, a mass flow rate of 7% of the original value is enough to prevent the coolant temperatures from ever rising above normal operating temperatures. This value was calculated by simulating only decay heat in the core and finding the minimum coolant mass flow rate that removes enough heat to prevent coolant or fuel failure.

**Table 13:** Complete Loss of Power Accident Summary

| | BOL | BOC | EOC |
|---|---|---|---|
| Time Until Coolant Boiling (seconds) | 117 | 117 | 117 |
| Time Until Fuel Melting (seconds) | 131 | 131 | 131 |

### *4.4 Different Axial Peaking Factors*

Using different axial power peaking factors in the SABR accident calculations changes very little. Because the total power produced across the fuel rod is the same, regardless of the peaking factor, the same amount of heat is going into each of the fuel pin elements. Outlet temperatures are no more than one degree Kelvin different for a perfectly sinusoidal axial power distribution, which has a peaking factor is $\pi/2$, and a much smaller peaking factor

such as 1.2. Even during accidents, the total power generated is constant for all peaking factors and thus the total heat coming out of the fuel pin is constant. The only thing that changes for different axial peaking factors is the location of the maximum temperature across the fuel pin elements. For flatter power distributions, the maximum temperature for the cladding and gap may be located at the outlet of the core. For highly peaked power distributions, the maximum temperature for the fuel pin, cladding and gap will be located before the outlet of the core. The maximum temperature for the coolant still occurs at the outlet to the core, regardless of the axial power peaking factor.

## *4.5 Accident Summary*

The easiest accidents to deal with are accidents affecting the neutron population in the fission core. Due to the plasma ion density limitations provided by the Troyon Beta Limit, it is highly unlikely for an accidental increase in plasma auxiliary heating to cause damage to SABR. Any increase in plasma auxiliary heating large enough to lead to fuel melting or coolant boiling will be preceded by thiss density limit being surpassed and a loss of plasma confinement in the neutron source.

Accidental increases in the ion fueling rate are also incapable of leading to reactor failure because the plasma is operating very close to the Troyon Beta Limit. During BOL, the plasma is operating at only 80% of the Troyon Beta Limit but operation during BOC and EOC is much closer to the ion density limit. Unfortunately, the fusion neutron source operating very close to this density limit provides very little margin against MHD instabilities. There is a wide range of operating parameters that could be used to achieve the desired fusion power output at BOL but for BOC and especially EOC operation, the range of operating parameters is smaller and does not provide much distance from the Troyon Beta Limit. To operate further away from these MHD instabilities it would be necessary to optimize the plasma current profile to allow for a significantly higher Troyon Beta Limit and more stability of SABR's fusion neutron source.

Because the fuel composition in SABR is designed with a maximum $k_{eff}$ of 0.95, any removal of control rods must occur at a level of multiplication lower than 0.95. Even if the

fusion neutron source is increased to account for this lower level of multiplication and the control rods are then removed, neither the coolant nor the fuel will fail. SABR's magnets and shielding regions also provide an added layer of security in that it is nearly impossible to insert enough positive reactivity in the form of additional fuel or neutron reflection into the core during operation without disrupting the fusion neutron source and thus shutting down the reactor.

Initiating events affecting SABR's heat removal systems are harder to deal with because there are no natural feedbacks to shut the reactor down in the event of one of these accidents. Loss of Flow Accidents due to any change in the coolant pumping power can quickly lead to coolant boiling and fuel melting if the coolant flow rate is not returned to a safe level. SABR can sustain up to a 49% LOFA without control action before the sodium boils. For small and medium LOFA, there will be many tens of seconds up to two and a half minutes before damage to the core results. Larger accidents will lead to coolant and fuel failure quicker and in the absolute worst case of a complete loss of flow, there are only 24 seconds before coolant failure. However, as stated earlier, a complete loss of flow is unrealistic as natural circulation will always exist.

The best way to deal with a Loss of Flow Accident is to first shut down the plasma by turning off the auxiliary heating drives. The remaining power production will be due to decay heat and as long as the flow rate is above 7% of its original value, SABR can effectively remove the remaining power being produced in the fission core. Any flow rate lower than 7% would require the use of auxiliary generators to power the coolant pumps. Because of the speed with which the plasma can be turned off, risk of reactor damage during Loss of Flow Accidents can be easily averted.

During a Loss of Heat Sink Accident, coolant in the primary loop will first boil for a 33% reduction in the overall heat transfer coefficient of the heat exchanger with 65 seconds to take corrective measures. As with a Loss of Flow Accident, the first step in dealing with a LOHSA is shutting down the plasma by turning off the auxiliary heating to the plasma. Once decay heat is the only power being produced in the core, a LOHSA is more easily dealt with. As long as the overall heat transfer coefficient of the heat exchanger

does not drop below 30% of its original value, the decay heat can be removed effectively. However, if there is a break in the intermediate loop and sodium is lost, more sodium cannot simply be pumped in. Back-up and emergency heat exchangers, such as sodium-to-air heat exchangers, working on separate coolant loops will be responsible for removing the power generated by decay heat in the event of a complete or nearly complete loss of heat sink.

For Loss of Power Accidents, decay heat will cause coolant boiling and fuel melting after two and a half minutes but this should be enough time to turn on auxiliary generators to run the pumps. Because a LOPA will nearly instantaneously shut down the plasma, fission power will decay away very quickly leaving only decay heat. If the coolant pumps are restarted in time, irreparable damage to SABR can be avoided. After the pumps are restarted, they must be kept online for at least a day until the decay heat becomes low enough to pose little risk. With careful monitoring of the coolant flow rate and quick response to turn on generators to run the coolant pumps, a Loss of Power Accident can be effectively and safely dealt with.

The first step in any accident scenario is to turn off the auxiliary heating to the plasma. Because of the large degree of subcriticality in the fission core, removing the source neutrons will cause the power produced in the reactor to decrease down to decay heat levels within a few seconds. Once SABR is producing only decay heat, back-up and emergency systems must be able to remove the remaining power produced in the fission core. In any event that the maximum coolant temperature rises above the 1,040 K, corrective measures should be taken immediately.

A limit on the coolant temperature of 1,040 K, which is the average of the boiling and normal operating temperatures, would be a good indication that a serious accident is taking place. For a Loss of Flow Accident, this temperature would correspond to a 36% decrease in the coolant mass flow rate. A 7% increase in the plasma ion fueling rate would lead to a coolant outlet temperature of 1,040 K. For BOL operation this constraint is reached before the Troyon Beta Limit is reached and leads to a loss of plasma confinement in the fusion neutron source. A 21% Loss of Heat Sink Accident corresponds to a coolant outlet temperature of 1,040 K. If the auxiliary heating were to be shut down at this coolant outlet

temperature for all accidents, the decay heat would be the only remaining issue.

# CHAPTER V

# CONCLUSIONS

Possible transients occurring in SABR can be placed into two different categories. The first category of transients is accidents affecting SABR's neutron population in the fission core, against which SABR is safe. Due to operation very close to the Troyon Beta Limit, SABR is inherently safe against accidental increases in the plasma ion fueling rate and plasma auxiliary heating. SABR is also inherently safe from any accidental control rod ejections due to the large degree of subcriticality. The second category of transients is those affecting SABR's heat removal systems: Loss of Flow, Heat Sink and Power Accidents. In all of these accidents, there are at least 10 seconds to respond to an initiating event by turning off the plasma auxiliary heating. This is probably not enough time to react by turning off the plasma auxiliary heating but it is, however, the absolute worst case scenario and does not take into natural circulation or secondary coolant loop flow coast down times. In more realistic accident scenarios, there are many tens of seconds up to a couple minutes for taking corrective measures before the coolant begins to boil and the fuel begins to melt. This required reaction time is less than ideal and requires careful monitoring of the temperature and power levels in the reactor but it should provide sufficient time for reactor operators to take action. After the plasma is shut down, if the coolant flow rate and heat exchanger continue to decrease, back-up pumps and heat exchangers must be turned on to remove the power produced by decay heat.

Because of the large positive sodium voiding and lack of $^{238}$U in the TRU fuel, SABR has a positive reactivity feedback. Due to this positive reactivity feedback and decay heat production, SABR will fail in the absence of external counter measures during severe accidents in the heat removal system. The subcritical nature of the reactor, however, provides a considerable margin of safety for dealing with this positive reactivity feedback during

transients. The immediate risk that all accidents pose can be diminished if the fusion neutron source is rapidly shut down leaving only decay heat to deal with. Because back-up and auxiliary pumps and heat exchangers will be responsible for providing sufficient heat removal, SABR requires further design of the primary, intermediate and secondary coolant loops so that a more in depth analysis can determine if the reactor is in fact safe from the worst case accident scenarios. Further work also should include separate systems dedicated to removing decay heat. However, for all accidents suggested in this thesis, there are viable options for preventing permanent damage to the reactor that make SABR, with additional design, a potential second generation Advanced Burner Reactor for minimizing the amount of Spent Nuclear Fuel that must be stored in High Level Waste Repositories.

# REFERENCES


[1] *Proc. 1st through 5th NEA International Exchange Meetings*. Paris, 1990, 1992, 1996, 1998, 2000, 2002, 2004, 2006. Nuclear Energy Agency, NEA/OECD.

[2] "Expected new nuclear power plant applications." http://www.nrc.gov/reactors/new-licensing/new-licensing-files/expected-new-rx-applications.pdf, March 2008.

[3] "International thermonuclear experimental reactor." http://www.iter.org, March 2008.

[4] "Nuclear Waste: Amounts and O-Site Storage." http://www.nei.org/, March 2008.

[5] Bosch, H. S. and Hale, G. M., "Improved Formulas for Fusion Cross-Sections and Thermal Reactivities," *Nuclear Fusion*, vol. 32, no. 4, 1992.

[6] Ertaud, A., *Superphénix*. Novatome, 1985.

[7] Hoffman, E. A. and Stacey, W. M., "Comparative Fuel Cycle Analysis of Critical and Sub-Critical Fast Reactor Transmutation Systems," *Nuclear Technology*, vol. 144, no. 83, 2003.

[8] Incropera, F. P. and DeWitt, D. P., *Fundamentals of Heat and Mass Transfer, Fifth Edition*. Hoboken, NJ: John Wiley & Sons, 2002.

[9] J. P. Floyd, e. a., "Tokamak Fusion Neutron Source for a Fast Transmutation Reactor," *Fusion Science & Technology*, vol. 52, pp. 727–730, October 2007.

[10] J.F. Briesmeister, E., *MCNP - A General Monte Carlo N-Particle Transport Code, Version 5*. Los Alamos National Laboratory, 2003.

[11] Kloosterman, J. and Kuijper, J., "VAREX, a Code for Variational Analysis of Reactivity Effects: Description and Examples," in *PHYSOR 2000*, (Seoul, South Korea), Delft University of Technology, October 2000.

[12] Kupitz, M. J., "Tecdoc-626: Safety Related Terms for Advanced Nuclear Plants," tech. rep., International Atomic Energy Agency, September 1991.

[13] Oak Ridge National Laboratory/U.S. Nuclear Regulatory Commission, *SCALE: A Modular Code System for Performing Standardized Computer Analyses for Licensing Evaluation*, March 1997. NUREG/CR-0200, Rev. 5 (ORNL/NUREG/CSD-2/R5), Vold. I, II, and III.

[14] Royl, P., Cramer, M., Plinate, P., and Natta, M., "Science and Technology of Fast Reactor Safety, Volume 1. Parametric SAS3D Simulations of the Superphnix-1 Type," (London), May 1986. British Nuclear Energy Society.

[15] S. Ukai, e. a., "R&D of Oxide Dispersion Strengthened Ferritic Martensitic Steels for FBR," *Journal of Nuclear Materials*, vol. 1745, pp. 258–263, 1998.

[16] Stacey, W. M., *Nuclear Reactor Physics*. New York: John Wiley & Sons, 2001.

[17] Stacey, W. M., *Fusion Plasma Physics*. Weinheim: Wiley-VCH Verlag GmbH & Co. KGaA, 2005.

[18] Todreas, N. E. and Kazimi, M. S., *Nuclear Systems I: Thermal Hydraulic Fundamentals, Second Printing*. London: Taylor & Francis, 1993.

[19] Ukai, S. and Fujiwara, M., "Perspective of ODS Alloys Application in Nuclear Environments," *Journal of Nuclear Materials*, vol. 749, pp. 307–311, 2004.

[20] W. M. Stacey, e. a., "A TRU-Zr Metal Fuel, Sodium Cooled, Fast Subcritical Advanced Burner Reactor," *Nuclear Technology*, vol. 162, pp. 53–79, April 2008.